2014

Effects of prey metapopulation structure on the viability of black-footed ferrets in plague-impacted landscapes: a metamodelling approach

Kevin Shoemaker
Stony Brook University

Robert Lacy
Chicago Zoological Society

Michelle Verant
USGS National Wildlife Health Center

Barry Brook
University of Adelaide

Travis Livieri
Prairie Wildlife Research

See next page for additional authors

50 YEARS WITH IMPACT
Journal of Applied Ecology
1913 2013 British Ecological Society CELEBRATING 100 YEARS

Journal of Applied Ecology 2014, **51,** 735–745 doi: 10.1111/1365-2664.12223

Effects of prey metapopulation structure on the viability of black-footed ferrets in plague-impacted landscapes: a metamodelling approach

Kevin T. Shoemaker[1], Robert C. Lacy[2], Michelle L. Verant[3], Barry W. Brook[4], Travis M. Livieri[5], Philip S. Miller[6], Damien A. Fordham[4] and H. Resit Akçakaya[1]*

[1]*Department of Ecology and Evolution, Stony Brook University, Stony Brook, NY 11794, USA;* [2]*Chicago Zoological Society, Brookfield, IL 60513, USA;* [3]*USGS National Wildlife Health Center, Madison, WI 53711, USA;* [4]*Environment Institute and School of Earth and Environmental Sciences, University of Adelaide, Adelaide, SA 5000, Australia;* [5]*Prairie Wildlife Research, Wellington, CO 80549, USA; and* [6]*IUCN SSC Conservation Breeding Specialist Group, Apple Valley, MN 55124, USA*

Summary

1. Species interactions have been largely ignored in extinction risk assessment. However, the black-footed ferret *Mustela nigripes* exemplifies a class of endangered species for which strong species interactions cannot be ignored. This species is an obligate predator of prairie dogs *Cynomys* spp., and sylvatic plague *Yersinia pestis* epizootics threaten to undermine recovery efforts by functionally eliminating the prey base. Multispecies 'metamodelling' techniques offer new opportunities for exploring population dynamics under strong species interdependencies and disease.

2. To investigate ferret extinction risk in plague-affected landscapes, we simultaneously modelled plague epidemiological processes, prairie dog metapopulation dynamics and ferret demographic responses. Ferret population dynamics were investigated at an important release site (Conata Basin in South Dakota) and for 500 artificial prey landscapes spanning a wide range of realistic colony configurations (e.g. total area, # colonies, spatial clustering) and demographic characteristics.

3. Our simulation models indicate that ferrets are unlikely to persist through episodes of plague at Conata Basin unless they can access prey resources from a wider region or unless management actions can otherwise substantially reduce plague transmission.

4. We show that large, diffuse prairie dog metapopulations (those with colonies spread over a region >2500 km^2) are most likely to support ferret populations in plague-affected landscapes. Our results also highlight the potential importance of metapopulation connectivity in fuelling plague epizootics and thereby imperilling black-footed ferret conservation efforts.

5. We describe a cycle (*c.* 5- to 25-year period) of plague-driven population crashes that is an emergent property of our models, and which can destabilize ferret populations.

6. *Synthesis and applications*. On the basis of our models, we conclude that few North American prairie dog complexes cover sufficient land area to sustain black-footed ferret populations through plague-driven crashes in prey abundance. Consequently, our results underscore the importance of working with many constituents to conserve large prairie dog landscapes in addition to continued development of plague mitigation tools. In addition, the strong relationship between plague-induced oscillatory prey cycles and predator population persistence highlights the potential conservation benefits of imposing strategic barriers to connectivity in areas over which plague outbreak cycles are strongly synchronous.

Key-words: connectivity, disease spread, oscillatory population dynamics, predator–prey interactions, sensitivity analysis, spatial structure

*Correspondence author: E-mail: Resit.Akcakaya@stonybrook.edu

Introduction

Species interactions underpin ecological theory and research, yet they have been largely ignored in extinction risk assessment (Soulé *et al.* 2005; Sabo 2008; Chadès, Curtis & Martin 2012). Failure to consider such feedbacks in conservation biology is particularly notable in the case of population viability analysis (PVA), a set of widely applied simulation modelling techniques for assessing extinction risk and exploring management options (Burgman, Ferson & Akçakaya 1993; Morris & Doak 2002). Typically, PVA models treat populations as isolated single-species systems (but see Fordham *et al.* 2013 for a recent exception), with interspecific interactions grouped with other external forcing factors and handled either as constraints on population growth (e.g. constant mortality term) or as factors that contribute to environmental variability (Sabo 2008). Similarly, disease is usually incorporated within PVAs as one of several stochastic causes of mortality or occasionally as the cause of periodic catastrophes (e.g. Frick *et al.* 2010). However, in reality, diseases have their own dynamics that are often strongly determined by demographic characteristics of their hosts (McCallum & Dobson 1995; Smith, Acevedo-Whitehouse & Pedersen 2009). As with other species interactions, the full interactive dynamics of epizootic disease as a factor that can destabilize or extirpate small populations is rarely modelled explicitly in PVAs (but see Haydon, Laurenson & Sillero-Zubiri 2002).

The endangered black-footed ferret *Mustela nigripes* (Audubon & Bachman 1851), native to the North American shortgrass prairie, is an obligate predator of prairie dogs *Cynomys* spp. and also extensively uses prairie dog colonies and burrows as habitat (Clark 1989; Biggins *et al.* 2006a). The dependence of black-footed ferrets on this single prey species suggests that the tight coupling of population dynamics in these two species cannot be ignored in PVA models. Furthermore, given that epizootics of plague (in prairie dogs and ferrets) and distemper (in ferrets) eliminated the last wild population of ferrets in 1987 (Biggins, Livieri & Breck 2011b) and continue to threaten the persistence of reintroduced populations, there is a clear need to explicitly account for disease dynamics in any PVA for black-footed ferrets. Here, we build a linked predator–prey PVA model that directly accounts for important spatially explicit disease processes and which represents one of the first attempts to model the effects of trophic linkages and disease on an endangered species.

Throughout the 20th century, black-footed ferret populations declined due to human persecution of prairie dogs (e.g. poisoning, rangeland conversion) and sylvatic plague, an exotic flea-borne disease (caused by the bacterium *Yersinia pestis*) that is highly fatal to both prairie dogs and black-footed ferrets. Black-footed ferrets were extinct in the wild by 1987 after the last 18 individuals were removed for captive breeding (Clark 1989). Since then, more than 7000 black-footed ferrets have been raised in captivity, of which over 3500 have been released into the wild at 19 locations in eight US states, Mexico and Canada (Jachowski *et al.* 2011a; Livieri 2011). Four reintroduction sites are now considered self-sustaining with no further reintroductions required. However, the continued eastward spread of sylvatic plague (Barnes 1982; Abbott & Rocke 2012) has resulted in catastrophic declines in prairie dog populations (e.g. Gage & Kosoy 2005), threatening to undermine recovery efforts (Kotliar, Baker & Whicker 1999; Livieri 2006).

To investigate black-footed ferret population viability in a dynamic, plague-affected landscape, we combined a plague epidemiological model, a prairie dog metapopulation model and a ferret population model. Using this multispecies approach to PVA (Miller & Lacy 2003; Prowse *et al.* 2013), we were able to explore the consequences of strong species interactions in ways not possible using standard PVA methods. We demonstrate that successful black-footed ferret reintroduction efforts in plague-affected landscapes may require large and diffuse prairie dog complexes or management actions to substantially reduce plague transmission rates. Furthermore, these coupled simulations predict oscillatory dynamics in both prey and predator populations, driven by complex interactions between plague epizootics and population recovery in a heterogeneous landscape. We show that this emergent property, which would not have been forecast using a single-species approach, and which is consistent with observations, has important potential consequences for the conservation of black-footed ferrets.

Materials and methods

STUDY SITE: CONATA/BADLANDS REGION

Releases of black-footed ferrets to Conata Basin (located within Buffalo Gap National Grasslands in South Dakota, USA, covering *c.* 500 km^2) began in 1996, resulting in a self-sustaining ferret population of 335 animals by 2007 (Livieri 2006; Wisely *et al.* 2008). To assess the prey base for ferrets, black-tailed prairie dog *Cynomys ludovicianus* colonies across southwestern South Dakota (hereafter, Conata/Badlands region, covering *c.* 20 000 km^2) were mapped by the US Forest Service, Badlands National Park and South Dakota Game, Fish and Parks (Biggins *et al.* 2006b; Sidle, Johnson & Euliss 2001; Cooper & Gabriel 2005; see Appendix S1 in Supporting Information). We used the union of the mapped polygon boundaries from all surveys between 1996 and 2009 to define the spatial extent of all distinct prairie dog colonies within the Conata Basin (area of known black-footed ferret occupancy; Biggins *et al.* 2011a) and the larger Conata/Badlands region, resulting in a metapopulation of 1591 black-tailed prairie dog colonies ranging from 5 ha to *c.* 10 000 ha in size (median colony area of 16 ha; Appendix S1), of which 71 colonies were identified as part of the Conata Basin and thereby known to be immediately available as prey for the ferret population (Fig. S4-2).

MODELLING OVERVIEW

We developed and linked three separate models (Fig. 1): an individual-based epidemiological model that simulated epizootics of plague; a spatially explicit, age- and sex-structured, stochastic model of the prairie dog metapopulation, and an age- and sex-structured, stochastic, single-population model of black-footed ferrets. These three models are detailed in the following sections. The epidemiological model provided inputs for stochastic ('catastrophe') parameters of the prairie dog model. The total population size of the prairie dogs at each time step of each replicate of the model was used to calculate the carrying capacity of the black-footed ferret population.

EPIDEMIOLOGICAL MODELLING (SYLVATIC PLAGUE)

We developed an individual-based epidemiological model that simulated epizootics of plague spreading through a prairie dog colony (see Appendix S2). Although black-footed ferrets are highly susceptible to plague (Williams *et al*. 1994; Godbey, Biggins & Garelle 2006), we did not model the direct effects of plague on black-footed ferret populations for two reasons. First, our use of a spatially unstructured ferret population model was likely to overstate the direct effects of plague on the ferret population (all ferrets would be exposed to plague simultaneously), preventing subsequent analysis of emergent dynamics and effects of prey spatial structure. Secondly, an effective vaccine has been developed and is currently administered to captive and wild-born ferrets (Abbott & Rocke 2012). Thus, our study assumes that this programme continues to successfully prevent plague outbreaks in the ferret population.

Simulation of basic epidemiological processes in a prairie dog colony and reporting of disease states (Susceptible, Exposed, Infectious, or Recovered) and survivorship were carried out at a daily time step using the software Outbreak (version 1.0; Pollak *et al*. 2008). Outbreak models were initialized with a single infected prairie dog within a colony comprising 1000 individuals, and all simulations were run for 365 days. Although there is some evidence for resistance to *Y. pestis* in black-tailed prairie dogs (Pauli *et al*. 2006; Rocke *et al*. 2012), this process is not yet well understood and was not included in this model. Detailed output data from Outbreak were used to generate three summary statistics that were subsequently used for modelling prairie dog metapopulation dynamics: (i) overall survival rate in a plague outbreak year, (ii) probability of a potential disperser individual being a carrier of plague and (iii) the probability of a single infected individual initiating an epizootic (Appendix S2).

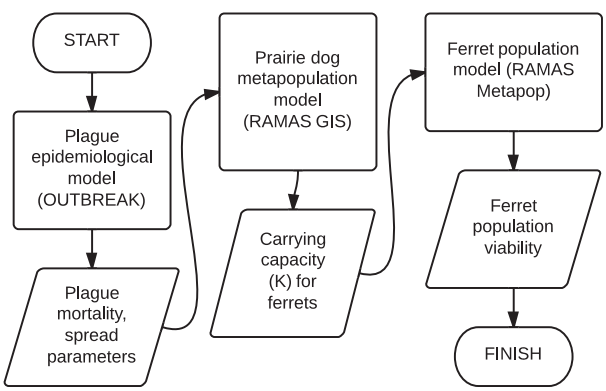

Fig. 1. Schematic flowchart of the metamodelling approach used in this study. Rectangular nodes represent processes (software in parentheses), and parallelogram nodes represent data output, which may be used as input for subsequent processes (indicated by arrows).

PRAIRIE DOG METAPOPULATION MODEL

We developed an age- and sex-structured matrix model for prairie dogs using RAMAS Metapop (Akçakaya & Root 2013), parameterized using data from Hoogland (1995, 2001, p. 377; Appendix S1). Density dependence was specified as a Ricker function, with a maximum annual population growth rate (R_{max}) of 2·44 (on the basis of populations recovering from plague outbreaks; Appendix S1). Each mapped colony was modelled as a distinct biological population, with carrying capacity (K) defined as a function of colony area and average densities of prairie dogs set at 28·7 ha^{-1}, on the basis of an estimate of prairie dog densities in the Conata region prior to the arrival of plague (Livieri 2006). Dispersal among prairie dog colonies was modelled as a function of inter-colony distances (Appendix S1), on the basis of data from Knowles, Proctor & Forest (2002), Lomolino & Smith (2001) and Garrett & Franklin (1988). We modelled plague dynamics within the prairie dog metapopulation as catastrophes spread by dispersers, with virulence (overall survival) and per-disperser probability of initiating an outbreak estimated from the epidemiological model (Fig. 1). All colonies were initialized at K and at stable age distribution, and all simulations were run with a 10-year burn-in period.

BLACK-FOOTED FERRET DEMOGRAPHIC MODEL

We developed an age- and sex-structured population projection matrix for the black-footed ferret, also using RAMAS Metapop, on the basis of a Wyoming mark–recapture study (Grenier, McDonald & Buskirk 2007) and the observed annual variability of the re-established ferret population in the Conata Basin (Livieri 2006; Appendix S1). On the basis of energetic considerations, we assumed that a population of 766 prairie dogs could sustain a single ferret (Stromberg, Rayburn & Clark 1983; Appendix S1). Thus, K for the ferret population was set at 1/766 of total prairie dog abundance at each time step. There is a great deal of uncertainty surrounding this estimate, which was derived under the simplifying assumptions that ferrets are monophagous consumers of prairie dogs and that prairie dog populations are exploited by no other major predator. However, although neither assumption is strictly true, violations of these two assumptions exhibit opposing biases, and therefore, no clear bias correction factor could be applied (see Appendix S1). Furthermore, an estimated ferret carrying capacity of 485 at Conata Basin, computed as 1/766 of estimated total prairie dog carrying capacity, is consistent with the observed growth of the reintroduced ferret population at Conata Basin, which appeared to plateau at abundances *c*. 350 prior to the arrival of plague in 2007 (Livieri 2006; Fig. S1-4). Due to the ferret's strong territorial behaviour, we capped the value of K during periods of high prairie dog densities to prevent ferret densities from exceeding 0·04 ferrets ha^{-1} (Biggins, Lockhart & Godbey 2006; Appendix S1). We used a Ricker (scramble) density dependence model, with R_{max} set at 1·48 on the basis of records from a rapidly growing Wyoming population

(Grenier, McDonald & Buskirk 2007; Appendix S1). Black-footed ferret abundance for each iteration was initialized using reintroduction records from Conata Basin (Livieri 2006).

We ran the black-footed ferret population model assuming either (i) ferrets could only access prairie dog colonies within the Conata Basin or (ii) ferrets could access all 1591 colonies within the larger Conata/Badlands region. Plague outbreaks were initiated in year 11 in a single large, centrally located colony within Conata Basin, reflecting ten plague-free years following the first ferret introductions (Abbott & Rocke 2012). We tested two alternative plague spread scenarios: (i) plague spreads only via prairie dog dispersal and (ii) plague outbreaks arise spontaneously with a probability of 0·05% per year per colony (resulting in a spontaneous plague initiation somewhere in the metapopulation nearly every other year and representing long-distance spread by alternative spread vectors such as coyotes and raptors). Ferret population viability was summarized using two metrics: quasi-extinction risk (defined as the proportion of simulation runs falling below five individuals by the final year of the simulation) and expected minimum abundance (defined as the minimum post-plague abundance averaged across all simulations; McCarthy & Thompson 2001).

SPATIAL SENSITIVITY ANALYSIS

To further investigate the effects of spatially explicit plague dynamics on ferret population viability, we ran the ferret population model with prey availability defined according to 500 distinct artificial prey landscapes. Simulation settings were varied across seven parameters hypothesized to influence the dynamics of plague spread (and thereby affect ferret population viability): (i) total landscape size (square areas varying from 30 km to 200 km per side), (ii) number of distinct colonies (varying from 9 to 1681), (iii) spatial clustering of colonies (regular grid or distinct clusters), (iv) background plague recurrence probability (plague spontaneously recurs somewhere in the metapopulation every 2 years to every 20 years), (v) prey $R_{\max}$ (varying from 1·8 to 2·8), (vi) intrinsic prey dispersal rate (intercept term from Eq. 1, varying from 0·061 to 0·105) and (vii) level of temporal variability in prey growth rate (see Appendix S3). Each of the 500 scenarios was selected by randomly sampling a single value from within the low-high range for each uncertain parameter (Table 1; Appendix S3). To study the effects of spatial configuration and fragmentation *per se* (Fahrig 2003), initial abundance and carrying capacity were set at two million individuals (approximating the initial estimated abundance of prairie dogs in the Conata/Badlands region) for all scenarios, representing sufficient prey resources to support a robust population of over 2000 black-footed ferrets in the absence of plague.

We assessed the relative importance of each variable as a predictor of black-footed ferret population viability using a Random Forest algorithm (Breiman 2001; Appendix S3). Relationships were visualized with conditional inference trees (Hothorn, Hornik & Zeileis 2006) and bivariate scatterplots. We also assessed the relationship between ferret population viability and mean nearest-neighbour distance among colonies in artificial prey landscapes, a derived variable closely related to landscape connectivity due to its role in determining prairie dog dispersal rates (and thereby affecting plague transmission risk; Appendix S3). To assess univariate relationships between sensitivity analysis variables and ferret population viability, we also fitted logit-linear models of ferret extinction risk as a function of each predictor variable.

After observing unexpected emergent oscillatory dynamics in the Conata/Badlands model and in many of the artificial prey landscapes, we assessed the contribution of each predictor variable (Table 1) to the emergence of oscillatory dynamics and the amplitude and frequency of the oscillations using the analytic approach outlined above (see Appendix S3). To assess the potential role of plague-driven oscillatory cycles in destabilizing ferret populations, we also examined the correspondence between ferret population viability and the occurrence of oscillations.

Results

EPIDEMIOLOGICAL MODEL

From the Outbreak output (n = 1000 replicates), we estimated that a single exposed prairie dog disperser had a 97% chance of initiating a plague epizootic in the

Table 1. Hypothesized influence of seven prairie dog metapopulation parameters on black-footed ferret population viability in artificial prey landscapes

Prairie dog variable	Range of values (see Table S3-1)	Hypothesized influence on black-footed ferret population viability
Metapopulation size (number of distinct colonies)	9–1681	More populations spread the risk of prey extinction.
Landscape size (km per side)	30–200	Larger and more diffuse landscapes will correspond to higher ferret viability via lower connectivity and plague transmission rates (e.g. McCallum & Dobson 2002).
Spatial clustering of colonies	Gridded, clustered	Clustered prairie dog landscapes will enable persistence of ferrets in smaller landscapes than gridded landscapes, by reducing global connectivity (and thereby plague transmission) relative to an equivalent gridded landscape.
Mean period of spontaneous plague outbreak recurrence	2–20	Presence of multiple plague initiation events (average of 1 colony every 2 years) will reduce ferret viability relative to single plague initiation event.
Intrinsic dispersal ability	0·061–0·105	Higher dispersal tendencies will result in more plague transmission events and therefore will lower ferret viability.
R_{max}	1·8–2·8	Higher R_{max} will correspond to faster recovery from plague and therefore higher ferret viability.
Temporal fluctuations in vital rates	See Table S1-1	Higher temporal variability will increase risk of ferret extinction after plague episodes, when ferret (and prey) abundance is lowest.

receiving colony. Once a plague epizootic was initiated, only 2·9% of the population survived to the next year (SE 0·8%). Averaged over an entire year, a prairie dog disperser from an infected colony had a 9·3% chance of carrying plague (see Appendix S1 for details on how we incorporated these results in the prey metapopulation model).

CASE STUDY: CONATA BASIN

Overall, the temporal pattern of plague prevalence (Fig. 2a,b) and prairie dog abundance (Fig. 2c,d) differed little between Conata Basin and the larger Conata/Badlands region. However, post-plague prairie dog abundance within the Conata Basin nearly always descended below levels capable of supporting a black-footed ferret population (Fig. 2c,e), whereas the ferret population tended to persist if available prey resources included all mapped colonies in the Conata/Badlands region (Fig. 2e). Simulated prairie dog (and ferret) population trajectories for the Conata/Badlands region frequently exhibited strong emergent oscillatory dynamics (Fig. S4-4). This cyclic pattern was not observed in the absence of spatial structure or sylvatic plague outbreaks (Fig. 3a,b). In models without explicit spatial structure (i.e. all colonies treated as a single panmictic population), prairie dog abundance crashed almost instantaneously (Fig. 3b), sharply contrasting with observed rates of plague spread in the Conata/Badlands region (plague took 3 years to travel *c.* 38 km; Travis M. Livieri, unpublished data). Rates of spread in spatially explicit models with a background rate of infection were consistent with the observed rate of spread at Conata Basin (Fig. S4-5). Limiting the initiation of plague to a single event resulted in a less frequent oscillatory pattern and higher mean prairie dog abundance (Fig. 3c) relative to scenarios with a background rate of infection due to occasional extirpation of plague from simulated landscapes (see link to plague spread animation in Appendix S4).

SPATIAL SENSITIVITY ANALYSIS

Black-footed ferret extinction risk was most sensitive to the spatial extent of artificial prairie dog metapopulations

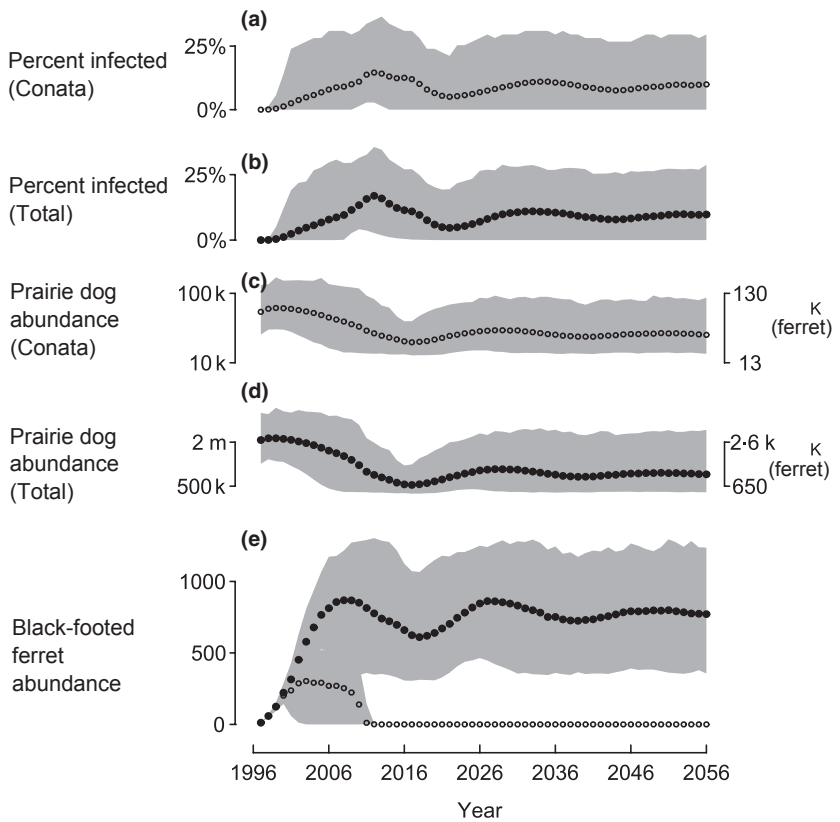

Fig. 2. Simulated abundance and infection rates for a plague-affected black-footed ferret study system in southwestern South Dakota. The top two panels illustrate regional plague severity (% of populations infected each year) for (a) the area observed to be used by ferrets (Conata Basin, open circles) and (b) the region potentially available to ferrets (Conata/Badlands region; filled circles). The next two panels display the simulated abundance of prairie dogs (c) in the Conata Basin area and (d) in the Conata/Badlands region. Secondary *y* axes display carrying capacity (*K*) for black-footed ferrets, computed as 1/766 of prairie dog abundance (see text). The final panel (e) displays simulated abundance of ferrets under two scenarios: *K* determined on the basis of prairie dog abundance in the Conata Basin (open circles), and *K* determined on the basis of prairie dog abundance in the larger Conata/Badlands region (filled circles). Ferret abundance starts from zero in the year 2000, the year ferret reintroduction began in the Conata Basin. Grey regions encompass 95% of the results from all simulation runs.

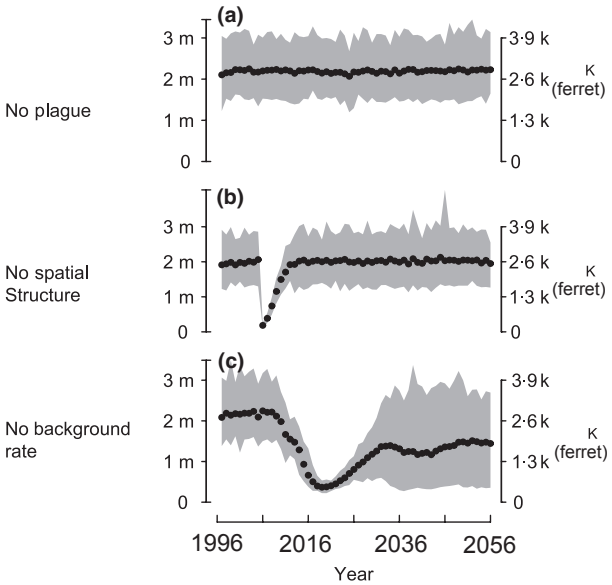

Fig. 3. Simulation results (total abundance of prairie dogs; cf. Fig. 2d) from the same model presented in Fig. 2, but run in the absence of (a) plague, (b) metapopulation structure (i.e. a single panmictic prairie dog population) and (c) background rate of plague (small probability of spontaneous infection), respectively.

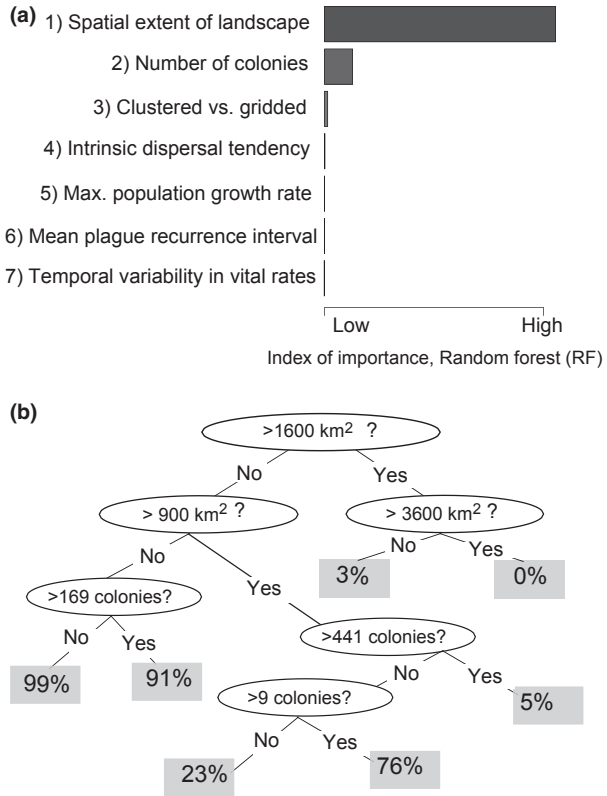

Fig. 4. Sensitivity of black-footed ferret extinction risk to seven variables hypothesized to influence the dynamics of plague spread in artificial prey landscapes: landscape extent, metapopulation size (number of colonies), spatial clustering of prairie dog colonies, intrinsic tendency of prairie dogs to disperse, maximum population growth rate (R_{max}), mean period between spontaneous plague recurrence and magnitude of annual fluctuations in prairie dog population growth. (a) Relative importance of each variable for predicting ferret extinction risk, derived from a Random Forest algorithm; (b) results from a single conditional inference tree. Splitting rules are indicated within ovals, and final predictions of extinction risk are shaded in grey.

(Fig. 4a), such that landscapes smaller than 50 × 50 km (2500 km^2, corresponding to regional densities >8 prairie dogs per ha) were less likely to sustain reintroduced ferret populations through plague epizootics (Figs 4b and 5a). The total number of colonies in the landscape ranked second in importance as a predictor of black-footed ferret extinction risk (Fig. 4a). The degree of fragmentation (# distinct colonies) and the configuration of colonies (gridded vs. clustered) influenced ferret viability for relatively dense prey landscapes (≤40 km per side), such that extinction risk was maximized at an intermediate level of fragmentation ($9 < \#$ colonies ≤ 441; Fig. 4b). The remaining variables included in the sensitivity analysis – presence of periodic plague initiation events, maximum intrinsic rate of growth of the prairie dog populations and the strength of temporal variation in prairie dog vital rates – had little detectable impact on black-footed ferret population viability (Fig. 4a). Landscape spatial extent exhibited a stronger association with black-footed ferret extinction risk than mean nearest-neighbour distance (mean distance from colony centre to nearest-neighbouring colony edge). A univariate logit-linear model of ferret extinction risk as a function of landscape extent (Fig. 5a) outperformed an analogous model with mean nearest-neighbour distance (Fig. 5b) with ΔAIC of 160. The observation that total landscape extent was a superior predictor of ferret extinction risk compared with mean nearest-neighbour distance (Fig. 5) suggests that plague spread was driven by the absolute numbers of dispersers rather than dispersal rates *per se*.

Prairie dog metapopulations with strong oscillatory dynamics generally corresponded to reduced ferret viability; expected minimum ferret abundance averaged 261 (95% CI: 244–278) in the absence of oscillatory cycles and 110 (95% CI: 79–140) in simulated landscapes with strong oscillatory cycles (Fig. 6a) across all 500 simulations in the spatial sensitivity analysis. Similarly, extinction risk increased from 0·08 (95% CI: 0·05–0·10) to 0·42 (95% CI: 0·34–0·50) in the presence of strong oscillations in landscape-level prairie dog abundance. When plotted across a two-dimensional slice of parameter space defined by the two highest importance variables for predicting ferret extinction risk (landscape extent and number of colonies), regions of high oscillation probability overlapped substantially with regions of high ferret extinction risk (Fig. 6b).

Discussion

Our modelling results suggest that black-footed ferret extinction risk may be higher in plague-affected landscapes

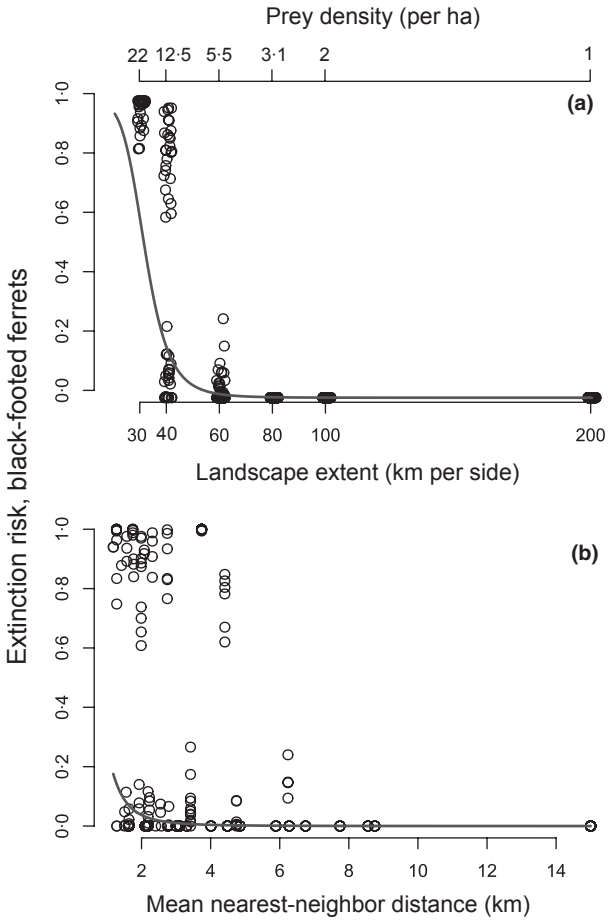

Fig. 5. Black-footed ferret extinction risk as a function of (a) spatial extent of artificial prey landscape (km per side) and (b) mean nearest-neighbour distance among colonies (km). For clarity, simulated landscapes with clustered colony structure are excluded.

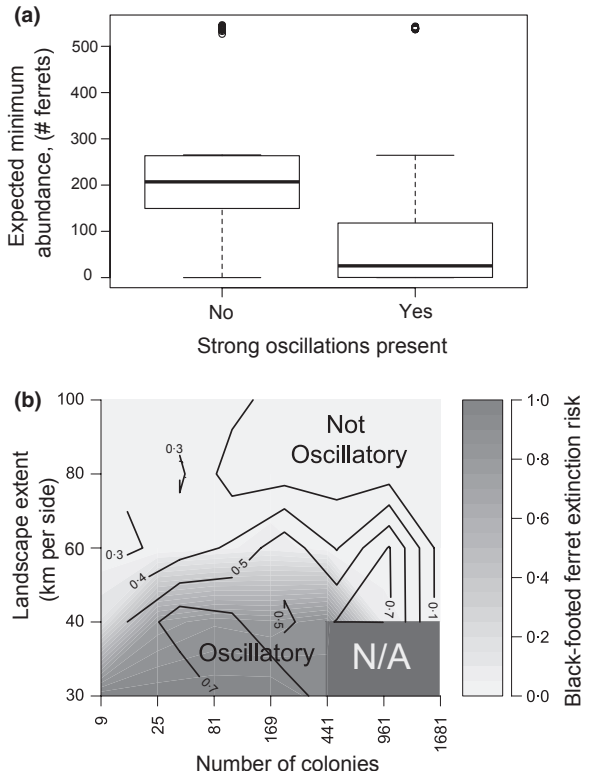

Fig. 6. Relationship between ferret population viability and the presence of strong plague-driven oscillatory dynamics in artificial prey landscapes. (a) expected minimum abundance for ferrets occupying prairie dog metapopulations with weak or no oscillatory dynamics (labelled 'No') vs. metapopulations with strong oscillatory dynamics (labelled 'Yes'). (b) Oscillatory dynamics and ferret extinction risk across a two-dimensional slice of parameter space covering a wide range of landscape sizes (km per side) and metapopulation sizes (number of colonies). Dark grey areas denote high risk of black-footed ferret extinction, and contour lines show the frequency of strong plague-driven oscillatory dynamics. The grey region labelled 'N/A' represents a constrained region of parameter space (i.e. unable to fit further distinct colonies without colony overlap).

with dense, closely spaced prairie dog colonies than in landscapes with colonies spread over larger areas (<8 prairie dogs ha^{-1} and covering >2500 km^2). Conata Basin, deemed high-quality habitat for reintroduced black-footed ferrets due to its large and densely packed black-tailed prairie dog colonies (Jachowski *et al*. 2011b; Livieri & Anderson 2012), provides an interesting case in point. This site was plague-free until 2008 and displayed growing or stable population dynamics of prairie dogs and black-footed ferrets from the date of first release (1996) to the date of plague arrival (Livieri 2006; Wisely *et al*. 2008). With regional black-tailed prairie dog densities measured as high as 30 to 50 per hectare (Biggins *et al*. 2011a), Conata Basin falls into a high-risk zone according to our models, whereby plague-induced extinction of black-footed ferrets is predicted in the absence of exogenous influences (e.g. influx of prey, relocation of ferrets or costly plague mitigation efforts). In reality, the ferret population at Conata Basin has declined dramatically since sylvatic plague was detected in 2008, falling from 335 in 2007 to only 71 animals in 2012 (Travis M. Livieri, unpublished data). Plague mitigation efforts at Conata Basin, including vaccination of black-footed ferrets, dusting (i.e. insecticide treatment) of prairie dog burrows and experimental oral vaccination of prairie dogs (Abbott & Rocke 2012), have thus far helped to avert extirpation of ferrets at this important release site.

This study highlights the potential importance of metapopulation connectivity in fuelling plague epizootics and thereby imperilling black-footed ferret conservation efforts. Empirical evidence supports the link between metapopulation connectivity and disease spread in this predator–prey–disease system. White-tailed prairie dogs *Cynomys leucurus* tend to occur in lower densities than black-tailed prairie dogs (Hoogland 1995), and some research indicates that black-footed ferret populations established on large, low-density white-tailed prairie dog complexes may have higher probabilities of surviving a plague epizootic than ferret populations occupying higher-density black-tailed prairie dog complexes (Cully &

Williams 2001). Notably, the ferret population at Shirley Basin, Wyoming (Grenier, McDonald & Buskirk 2007), occupying a large (>1200 km^2) complex of white-tailed prairie dogs, persisted through a plague epizootic in 1994 (Wisely *et al*. 2008) without plague mitigation or other exogenous influences. Furthermore, evidence suggests that the last wild black-footed ferret population (at Meeteetse, Wyoming), also occupying white-tailed prairie dog habitat, experienced at least one plague epizootic prior to ferret extirpation (but plague ultimately led to the demise of this population). Nonetheless, plague currently affects populations of white-tailed, black-tailed, Gunnisons *C. gunnisoni* and Utah prairie dogs *C. parvidens* and the mechanisms underlying epizootics remain unclear, underscoring the need for continued research on plague persistence and transmission.

EMERGENT PATTERNS

Our study highlights the interesting demographic dynamics that can emerge in a spatially complex landscape with density-dependent, disperser-mediated disease transmission. Among the emergent patterns observed in our simulation models, perhaps most notable was the oscillatory fluctuations in predator and prey abundance exhibited in the Conata Basin case study and many of the artificial prey landscapes. This oscillatory pattern was driven by disperser-mediated disease transmission, whereby plague epizootics were suppressed by insufficient transmission rates at low population densities. As prairie dog populations grew and connectivity was restored, a wave of renewed outbreaks of plague became inevitable, generating a cycle of collapse and recovery that could be sustained as long as *Y. pestis* persisted within the metapopulation (see link to animation in Appendix S4). Not surprisingly, the strongest oscillatory dynamics tended to correspond with compact, high-connectivity artificial landscapes in which plague could spread rapidly and synchronously through the prairie dog metapopulation (Fig. 6b). Similar cycles (5–10 years) of plague outbreaks have also been observed in natural systems (Barnes 1982; Cully & Williams 2001; Cully *et al*. 2010), although the underlying mechanisms are unclear. For example, an unmanaged black-tailed prairie dog colony at Rocky Mountain Arsenal National Wildlife Refuge has exhibited a *c*. 5-year interval between plague epizootics from 1988 to 2000 (Seery & Matiatos 2000; Seery *et al*. 2003).

ADVANTAGES AND DISADVANTAGES OF LINKED METAMODELS RELATIVE TO SINGLE-SPECIES MODELS

In this study, we used linked models – what has been termed a 'metamodel' approach (Miller & Lacy 2003; Lacy *et al*. 2013; Prowse *et al*. 2013) – to reveal dynamics that can emerge from interactions among species and with disease (Fig. 1). The oscillatory dynamics of prairie dog abundance, in turn driving oscillations and sometimes extinction of the ferret population, did not occur in models that lacked epidemic disease, spatial structure of the prairie dog metapopulation or occasional arrival of infected animals from outside the modelled system. Therefore, a more traditional single-species PVA model of the black-footed ferret population, even if incorporating the requirement for a sufficient prey base and the threat from occasional disease, would not have led to the same predictions regarding the importance of habitat extent in mediating the impact of epidemic disease on the predator–prey system.

However, there are also disadvantages of a metamodel compared to models that focus on one primary process or species. Each submodel requires many parameters that are at best uncertain. While a metamodel usefully allows dynamic processes to cascade through the linkages, the uncertainty also propagates. Therefore, sensitivity tests will be necessary to identify dependence of results on uncertain parameters (e.g. Figs 4, 5 and 6) as well as the dependence of results on metamodel structure (e.g. presence or absence of specific metamodel components; Fig. 3).

CAVEATS

We used sensitivity analysis to reveal which factors and processes in the model had largest effect on results and to test whether alternative estimates would have led to different general conclusions. However, we recognize that uncertain or omitted factors beyond the scope of our sensitivity analysis could alter simulation results and subsequent management recommendations. In our models, black-footed ferret populations behaved as a single panmictic group regardless of the size or spatial structuring of prey populations. However, spatial structuring of ferret populations may have important consequences for population viability via local prey deficiencies (potentially damaging viability) and extinction–recolonization dynamics (potentially conferring dynamic metapopulation stability; Hanski, Moilanen & Gyllenberg 1996). Although it is clear that black-footed ferret spatial ecology is strongly dependent on the spatial distribution of their primary prey (Jachowski *et al*. 2010; Eads *et al*. 2011), the conditions (e.g. spatial extent and clustering of prey colonies) under which metapopulation dynamics emerge in black-footed ferrets remain unclear. Black-footed ferrets are capable of long-distance movements and have been known to cover more than 49 km in short periods (Biggins *et al*. 1999). In Conata Basin, annual net displacement distances of 10 km by both males and females were documented (Travis M. Livieri, unpublished data), suggesting that it may not be unreasonable to assume that ferrets could occupy a 200 × 200 km prairie dog complex (largest artificial landscapes in this study) after 10 years. Clearly, the spatial ecology of ferret populations occupying heterogeneous, low-density prairie dog landscapes merits further research.

In our models, plague transmission among colonies primarily occurred via disperser-mediated transmission of infected fleas. However, carnivores and raptors are likely to play a role in transporting plague-infected fleas to distant prairie dog colonies (Abbott & Rocke 2012), and small mammals – notably, grasshopper mice *Onychomys leucogaster* – have been strongly implicated in plague spread at smaller spatial scales (Salkeld *et al.* 2010). However, the mechanisms of plague transmission among colonies by these organisms are not yet well understood, especially at large spatial scales. For simplicity, we modelled the composite contribution of alternative transmission vectors using a single constant background rate of infection. We also did not attempt to model enzootic plague, which affects both prairie dogs (Biggins *et al.* 2010) and black-footed ferrets (Matchett *et al.* 2010). We emphasize that very different demographic outcomes and management recommendations may emerge if alternative mechanisms were found to play a more dominant role in plague transmission. As additional data on plague transmission (and other demographic processes) become available at sites like Conata Basin, refined versions of our models can be used to produce robust site-specific management recommendations.

MANAGEMENT IMPLICATIONS

The recovery goal for black-footed ferrets, as stated in the current recovery plan (U.S. Fish & Wildlife Service 2013), is 3000 black-footed ferrets in 30 or more populations across the historic range. Our models suggest that vast prairie landscapes (>2500 km^2) may be necessary to sustain a single ferret population through recurring plague epizootics. Although other studies (Forrest *et al.* 1985; Richardson *et al.* 1986; US Fish & Wildlife Service 1988, 2013; Conservation Breeding Specialist Group 2004; Jachowski *et al.* 2011a) have also concluded that 'large' areas of habitat are necessary to maintain black-footed ferrets, the areas mentioned in these studies range only from 25 to 200 km^2. Unfortunately, few landscapes >2500 km^2 occupied by prairie dogs exist today (Proctor, Haskins & Forrest 2006). For the foreseeable future, it is likely that successful efforts to achieve recovery goals for black-footed ferrets in plague-affected areas will depend upon effective plague mitigation tools such as dusting of prairie dog burrows and vaccination of ferrets (Abbott & Rocke 2012). Extensive field trials of an oral prairie dog vaccine for prairie dogs are currently underway (T. E. Rocke, personal communication). In addition, the strong relationship between plague-induced oscillatory prey cycles and predatory population persistence, as suggested by our models (Fig. 6), suggests the use of field surveys to assess the spatial extent over which plague outbreak cycles are strongly synchronous. Targeting these high-risk areas with management interventions to disrupt connectivity and subsequent plague transmission may help to minimize the extent of plague epizootics and overall impact on the prairie dog metapopulation (Fig. S4-4) Our findings underscore the importance of working with many constituents to conserve large prairie dog landscapes (Proctor, Haskins & Forrest 2006; Jachowski *et al.* 2011a; Livieri 2011) and to develop improved plague mitigation tools. More generally, this study illustrates the insights that multispecies modelling yields for population viability assessment and conservation planning, especially for strongly interacting or co-dependent species ensembles that include threatened taxa.

Acknowledgements

This study was supported by NSF grant DEB-1146198. BWB was supported by Australian Research Council (ARC) grants DP120101019 and FT100100200. DAF was supported by ARC grant DP1096427 and ARC fellowship FS110200051. M. Aiello-Lammens wrote the R scripts for data exchange between R and RAMAS. Thanks to D.E. Biggins, M.R. Matchett and three anonymous reviewers for helpful comments and discussion.

Data accessibility

Detailed model descriptions are available in the online supporting information and R scripts are available from the authors upon request.

References

Abbott, R.C. & Rocke, T.E. (2012) *Plague: U.S. Geological Survey Circular 1372*, 79 p., plus appendix. (Also available at http://pubs.usgs.gov/circ/1372.)

Akçakaya, H.R. & Root, W. (2013) *RAMAS Metapop: Viability Analysis for Stage-Structured Metapopulations (Version 6.0)*. Applied Biomathematics, Setauket, New York.

Barnes, A.M. (1982) Surveillance and control of plague in the United States. *Animal Disease in Relation to Animal Conservation*. Symposia of the Zoological Society of London 50 (eds M.A. Edwards & U. McDonnell), pp. 237–270. Academic Press, New York.

Biggins, D.E., Livieri, T.M. & Breck, S.W. (2011b) Interface between black-footed ferret research and operational conservation. *Journal of Mammalogy*, **92**, 699–704.

Biggins, D.E., Lockhart, J.M. & Godbey, J.L. (2006) Evaluating habitat for black-footed ferrets: revision of an existing model. *Recovery of the Black-Footed Ferret – Progress and Continuing Challenges* (eds J.E. Roelle, B.J. Miller, J.L. Godbey & D.E. Biggins), pp. 143–150. U.S. Geological Survey, Scientific Investigations Report 2005-5293, Reston, VA

Biggins, D.E., Vargas, A., Godbey, J.L. & Anderson, S.H. (1999) Influence of prerelease experience on reintroduced black-footed ferrets (*Mustela nigripes*). *Biological Conservation*, **89**, 121–129.

Biggins, D.E., Godbey, J.L., Matchett, M.R. & Livieri, T.M. (2006a) Habitat preferences and intraspecific competition in black-footed ferrets. *Recovery of the Black-Footed Ferret – Progress and Continuing Challenges* (eds J.E. Roelle, B.J. Miller, J.L. Godbey & D.E. Biggins), pp. 129–140. U.S. Geological Survey, Scientific Investigations Report 2005-5293, Reston, VA.

Biggins, D.E., Sidle, J.G., Seery, D.B. & Ernst, A.E. (2006b) Estimating the abundance of prairie dogs. *Conservation of the Black-tailed Prairie Dog: Saving North America's Western Grasslands* (ed. J.L. Hoogland), pp. 94–107. Island Press, Washington, DC.

Biggins, D.E., Godbey, J.L., Gage, K.L., Carter, L.G. & Montenieri, J.A. (2010) Vector control improves survival of prairie dogs (*Cynomys*) in areas considered enzootic for plague. *Vector-Borne and Zoonotic Diseases*, **10**, 17–26.

Biggins, D.E., Godbey, J.L., Horton, B.M. & Livieri, T.M. (2011a) Movements and survival of black-footed ferrets associated with an experimental translocation in South Dakota. *Journal of Mammalogy*, **92**, 742–750.

Breiman, L. (2001) Random forest. *Machine Learning*, **45**, 5–32.

Burgman, M., Ferson, S. & Akçakaya, H.R. (1993) *Risk Assessment in Conservation Biology*. Chapman and Hall, New York.

Chadès, I., Curtis, J.M.R. & Martin, T.G. (2012) Setting realistic recovery targets for two interacting endangered species, sea otter and northern abalone. *Conservation Biology*, **26**, 1016–1025.

Clark, T.W. (1989) *Conservation Biology of the Black-footed Ferret Mustela nigripes*. Wildlife Preservation Trust Special Scientific Report No. 3, Wildlife Preservation Trust International, Philadelphia, PA, USA, 175 pp.

Conservation Breeding Specialist Group (2004) *Black-footed Ferret Population Management Planning Workshop. Final Report*. IUCN/SSC Conservation Breeding Specialist Group, Apple Valley, MN. 130pp.

Cooper, J. & Gabriel, L. (2005) *South Dakota Black-Tailed Prairie Dog Conservation and Management Plan*. South Dakota Department of Game, Fish and Parks and South Dakota Department of Agriculture, Pierre, South Dakota. 68p.

Cully, J.F. & Williams, E.S. (2001) Interspecific comparisons of sylvatic plague in prairie dogs. *Journal of Mammalogy*, **82**, 894–905.

Cully, J.F., Johnson, T.L., Collinge, S.K. & Ray, C. (2010) Disease limits populations: plague and black-tailed prairie dogs. *Vector Borne Zoonotic Disease*, **10**, 7–15.

Eads, D.A., Millspaugh, J.J., Biggins, D.E., Livieri, T.M. & Jachowski, D.S. (2011) Post-breeding resource selection by adult black-footed ferrets in the Conata Basin, South Dakota. *Journal of Mammalogy*, **92**, 760–770.

Fahrig, L. (2003) Effects of habitat fragmentation on biodiversity. *Annual Review of Ecology, Evolution, and Systematics*, **34**, 487–515.

Fordham, D.A., Akçakaya, H.R., Brook, B.W., Rodríguez, A., Alves, P.C., Civantos, E., Triviño, M., Watts, M.J. & Araújo, M.B. (2013) Adapted conservation measures are required to save the Iberian lynx in a changing climate. *Nature Climate Change*, **3**, 899–903.

Forrest, S.C., Clark, T.W., Richardson, L. & Campbell III, T.M. (1985) *Black-footed ferret habitat: some management and reintroduction considerations*. Wyoming Bureau of Land Management, Wildlife Technical Bulletin 2 Wyoming Bureau of Land Mangement, Cheyenne, WY. 49p.

Frick, W.F., Pollock, J.F., Hicks, A.C., Langwig, K.E., Reynolds, D.S., Turner, G.G. *et al*. (2010) An emerging disease causes regional population collapse of a common North American bat species. *Science*, **329**, 679–682.

Gage, K.L. & Kosoy, M.Y. (2005) Natural history of plague: perspectives from more than a century of research. *Annual Review of Entomology*, **50**, 505–528.

Garrett, M.G. & Franklin, W.L. (1988) Behavioral ecology of dispersal in the black-tailed prairie dog. *Journal of Mammalogy*, **69**, 236–250.

Godbey, J.L., Biggins, D.E. & Garelle, D. (2006) Exposure of captive black-footed ferrets to plague and implications for species recovery. *Recovery of the Black-Footed Ferret – Progress and Continuing Challenges* (eds J.E. Roelle, B.J. Miller, J.L. Godbey & D.E. Biggins), pp. 233–237. U.S. Geological Survey, Scientific Investigations Report 2005-5293, Reston, VA.

Grenier, M.B., McDonald, D.B. & Buskirk, S.W. (2007) Rapid population growth of a critically endangered carnivore. *Science*, **317**, 779.

Hanski, I., Moilanen, A. & Gyllenberg, M. (1996) Minimum viable metapopulation size. *American Naturalist*, **147**, 527–541.

Haydon, D.T., Laurenson, M.K. & Sillero-Zubiri, C. (2002) Integrating epidemiology into population viability analysis: managing the risk posed by rabies and canine distemper to the Ethiopian wolf. *Conservation Biology*, **16**, 1372–1385.

Hoogland, J.L. (1995) *The Black-Tailed Prairie Dog: Social Life of A Burrowing Mammal*. The University of Chicago Press, Chicago, IL.

Hoogland, J.L. (2001) Black-tailed, Gunnison's, and Utah prairie dogs reproduce slowly. *Journal of Mammalogy*, **82**, 917–927.

Hothorn, T., Hornik, K. & Zeileis, A. (2006) Unbiased recursive partitioning: a conditional inference framework. *Journal of Computational and Graphical Statistics*, **15**, 651–674.

Jachowski, D.S., Millspaugh, J.J., Biggins, D.E., Livieri, T.M. & Matchett, M.R. (2010) Home-range size and spatial organization of black-footed ferrets *Mustela nigripes* in South Dakota, USA. *Wildlife Biology*, **16**, 1–11.

Jachowski, D.S., Gitzen, R.A., Grenier, M.B., Holmes, B. & Millspaugh, J.J. (2011a) The importance of thinking big: large-scale prey conservation drives black-footed ferret reintroduction success. *Biological Conservation*, **144**, 1560–1566.

Jachowski, D.S., Millspaugh, J.J., Biggins, D.E., Livieri, T.M., Matchett, M.R. & Rittenhouse, C.D. (2011b) Resource selection by black-footed ferrets in South Dakota and Montana. *Natural Areas Journal*, **31**, 218–225.

Knowles, C., Proctor, J. & Forest, S. (2002) Black-tailed prairie dog abundance and distribution in the great plains based on historic and contemporary information. *Great Plains Research: A Journal of Natural and Social Sciences* Paper 608. http://digitalcommons.unl.edu/greatplainsresearch/608 (accessed 23 May 2012).

Kotliar, N.B., Baker, B.W. & Whicker, A.D. (1999) A critical review of assumptions about the prairie dog as a keystone species. *Environmental Management*, **24**, 177–192.

Lacy, R.C., Miller, P.S., Nyhus, P.J., Pollak, J.P., Raboy, B.E. & Zeigler, S. (2013) Metamodels for transdisciplinary analysis of wildlife population dynamics. *PLoS One*, **8**, e84211.

Livieri, T.M. (2006) *Ten-Year History of the Conata Basin Black-Footed Ferret Population: 1996–2005*. Prairie Wildlife Research, Wall, South Dakota. 49 p.

Livieri, T.M. (2011) Black-footed ferret recovery in North America. *Global Re-Introduction Perspectives: 2011. More Case Studies from Around the Globe* (ed. P. Soorae), pp. 157–164. IUCN/SSC Re-introduction Specialist Group and Abu Dhabi, UAE: Environment, Abu Dhabi, United Arab Emirates. 250p.

Livieri, T.M. & Anderson, E.M. (2012) Black-footed ferret home ranges in Conata Basin, South Dakota. *Western North American Naturalist*, **72**, 196–205.

Lomolino, M.V. & Smith, G.A. (2001) Dynamic biogeography of prairie dog (*Cynomys ludovicianus*) towns near the edge of their range. *Journal of Mammalogy*, **82**, 937–945.

Matchett, M.R., Biggins, D.E., Carlson, V., Powell, B. & Rocke, T. (2010) Enzootic plague reduces black-footed ferret (*Mustela nigripes*) survival in Montana. *Vector-Borne and Zoonotic Diseases*, **10**, 27–35.

McCallum, H.I. & Dobson, A.P. (1995) Detecting disease and parasite threats to endangered species and ecosystems. *Trends in Ecology & Evolution*, **10**, 190–194.

McCallum, H.I. & Dobson, A.P. (2002) Disease, habitat fragmentation and conservation. *Proceedings of the Royal Society of London Series B*, **269**, 2041–2049.

McCarthy, M.A. & Thompson, C. (2001) Expected minimum population size as a measure of threat. *Animal Conservation*, **4**, 351–355.

Miller, P.S. & Lacy, R.C. (2003) Metamodels as a tool for risk assessment. *Experiments in Consilience: Integrating Social and Scientific Responses to Save Endangered Species* (eds F.R. Westley & P.S. Miller), pp. 333–351. Island Press, Washington, DC.

Morris, W.F. & Doak, D.F. (2002) *Quantitative Conservation Biology. Theory and Practice of Population Viability Analysis*. Sinauer, Sunderland, MA.

Pauli, J.N., Buskirk, S.W., Williams, E.S. & Edwards, W.H.A. (2006) A plague epizootic in the black-tailed prairie dog (*Cynomys ludovicianus*). *Journal of Wildlife Diseases*, **42**, 74–80.

Pollak, J.P., Miller, P.S., Lacy, R.C., Hungerford, L. & Bright, P. (2008) *Outbreak Version 0.99*. IUCN SSC Conservation Breeding Specialist Group, Apple Valley, MN.

Proctor, J., Haskins, B. & Forrest, S.C. (2006) Focal areas for conservation of prairie dogs and the grassland ecosystem. *Conservation of the Black-Tailed Prairie Dog: Saving North America's Western Grasslands* (ed. J.L. Hoogland), pp. 232–247. Island Press, Washington, DC.

Prowse, T.A.A., Johnson, C.N., Lacy, R.C., Bradshaw, C.J.A., Pollak, J.P., Watts, M.J. & Brook, B.W. (2013) No need for disease: testing extinction hypotheses for the thylacine using multi-species metamodels. *Journal of Animal Ecology*, **82**, 355–364.

Rocke, T.E., Williamson, J., Cobble, K.R., Busch, J.D., Antolin, M.F. & Wagner, D.M. (2012) Resistance to plague among black-tailed prairie dog populations. *Vector-Borne and Zoonotic Diseases*, **12**, 111–116.

Richardson, L., Clark, T.W., Forrest, S.C. & Campbell, T.M. III (1986) Black-footed ferret recovery: a discussion of some options and considerations. *Great Basin Naturalist Memoirs*, **8**, 169–184.

Sabo, J.L. (2008) Population viability and species interactions: life outside the single-species vacuum. *Biological Conservation*, **141**, 276–286.

Salkeld, D.J., Salathé, M., Stapp, P. & Jones, J.H. (2010) Plague outbreaks in prairie dog populations explained by percolation thresholds of alternate host abundance. *Proceedings of the National Academy of Sciences USA*, **107**, 14247–14250.

Seery, D.B. & Matiatos, D.J. (2000) Response of wintering buteos to plague epizootics in prairie dogs. *Western North American Naturalist*, **60**, 420–425.

Seery, D.B., Biggins, D.E., Montenieri, J.A., Enscore, R.E., Tanda, D.T. & Gage, K.L. (2003) Treatment of black-tailed prairie dog burrows with Deltamethrin to control fleas (Insecta: Siphonaptera) and plague. *Journal of Medical Entomology*, **40**, 718–722.

Sidle, J.G., Johnson, D.H. & Euliss, B.R. (2001) Estimated areal extent of colonies of black-tailed prairie dogs in the northern great plains. *Journal of Mammalogy*, **82**, 928–936.

Smith, K.F., Acevedo-Whitehouse, K. & Pedersen, A.B. (2009) The role of infectious diseases in biological conservation. *Animal Conservation*, **12**, 1–12.

Soulé, M.E., Estes, J.A., Miller, B. & Honnold, D.L. (2005) Strongly interacting species. conservation policy, management, and ethics. *BioScience*, **55**, 168–176.

Stromberg, M.R., Rayburn, R.L. & Clark, T.W. (1983) Black-footed ferret prey requirements—an energy balance estimate. *Journal of Wildlife Management*, **47**, 67–73.

U.S. Fish & Wildlife Service (1988) *Black-footed ferret recovery plan*. U.S. Fish & Wildlife Service, Denver, Colorado.

U.S. Fish and Wildlife Service (2013) *Recovery Plan for the Black-Footed Ferret (Mustela nigripes)*. U.S. Fish and Wildlife Service, Denver, CO U.S.A.

Williams, E.S., Kwiatkowski, D.R., Thome, E.T. & Boerger-Fields, A. (1994) Plague in a black-footed ferret. *Journal of Wildlife Diseases*, **30**, 581–585.

Wisely, S.M., Santymire, R.M., Livieri, T.M., Mueting, S.A. & Howard, J. (2008) Genotypic and phenotypic consequences of reintroduction history in the black-footed ferret (*Mustela nigripes*). *Conservation Genetics*, **9**, 389–399.

Received 16 August 2013; accepted 14 January 2014
Handling Editor: Philip Stephens

Supporting Information

Additional Supporting Information may be found in the online version of this article.

Appendix S1. Demographic and spatial model specifications.

Appendix S2. Details of the plague transmission model.

Appendix S3. Details of the sensitivity analysis routine.

Appendix S4. Supplementary Results and Figures.

Kevin T. Shoemaker, Robert C. Lacy, Michelle L. Verant, Barry W. Brook, Travis M. Livieri, Phillip S. Miller, Damien A. Fordham, and H. Resit Akçakaya*. Effects of prey metapopulation structure on the viability of black-footed ferrets in plague-impacted landscapes: a metamodelling approach. *Journal of Applied Ecology.*

Supporting Information

Appendix S1: Demographic and spatial model specifications

Prairie Dog Metapopulation Model

Spatial structure of study region

The spatial structure of the metapopulation was based on the distribution of prairie dogs in the Conata Basin, a subset of 71 prairie dog populations within the Conata/Badlands region in South Dakota and covering ca. 500 km^2 (Fig. S4-2; delineated based on Biggins et al. 2011) is a portion of the Buffalo Gap National Grasslands directly south of Badlands National Park and is administered by the US Forest Service (Fig. S4-2). This area was chosen in the early 1990's for reintroduction of black-footed ferrets due to the extensive network of high-density prairie dog colonies located on public lands (Livieri 2006). As part of black-footed ferret reintroduction efforts, 150 captive-born ferret kits were released over a 4-year period to prairie dog colonies in Conata Basin beginning in 1996. This effort resulted in a self-sustaining population with an annual total of approximately 200 animals by the year 2000 (Livieri 2006). Plague-free prairie dog populations at Conata Basin contributed to rapid establishment of ferrets at this site, making it among the most successful ferret reintroduction sites and the largest reintroduced population of black-footed ferrets (335 individuals recorded in 2007). The black-footed ferret population at Conata Basin has declined dramatically since sylvatic plague was detected in 2008, falling from 335 individuals documented in 2007 to only 71 in 2012 (Livieri *2012*).To prevent extinction of the ferret population, plague mitigation efforts have recently been implemented, including dusting of prairie dog burrows and experimental vaccination of black-footed ferrets (Abbott and Rocke 2012).

Prairie dog colonies in Conata Basin, Badlands National Park, and Buffalo Gap National Grasslands in southwestern South Dakota, USA (hereafter, Conata/Badlands region) were mapped biennially by the US Forest Service and Badlands National Park from 1996-2009 using differentially corrected Global Positioning Systems (GPS) units to connect the outermost prairie dog burrows into a polygon (Biggins et al. 2006a). Prairie dog colonies in the surrounding areas were mapped in 2004 using aerial transects and digital imaging (Sidle et al. 2001, Cooper and Gabriel 2005). We converted prairie dog colony maps to binary (0=non-habitat, 1=habitat) raster maps with 50m cell size. We re-imposed barriers (e.g., roads, pipelines) that were lost in the rasterization process. We used the union of all years to define potential habitat. We used neighborhood distance of 1 cell (50m) to define the population structure (see Akçakaya 2002 for details of how the program determines spatial structure). Thus, we assumed each colony is a distinct biological population, which may be connected to other such populations (see section on dispersal below). Excluding very small colonies with carrying capacity (K) <100 (see below), this resulted in 1591 PD populations ranging from about 5 ha to 10,000 ha, with a median size of 16 ha and covering ca. 20,000 km^2 (Fig. S1-1). .

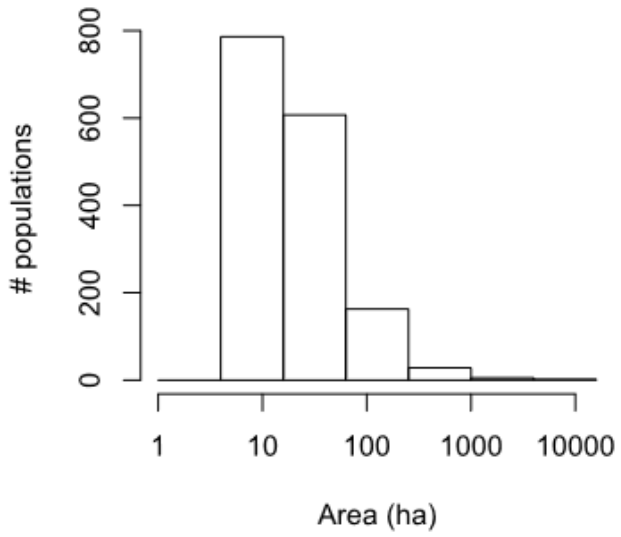

Fig. S1-1. Histogram of patch areas (ha) for all prairie dog habitat patches (n = 1591) identified in the Conata-Badlands region of South Dakota, based on mapped records of prairie dog colony boundaries.

Carrying capacity and density dependence

Reproduction in prairie dogs is often limited by resources (Hoogland 2001), suggesting a Ricker-type (scramble) density dependent effect on fecundities. We therefore used this type of density dependence, and estimated the maximum growth rate (R_{max}) based on the average of exponential growth rates exhibited by several populations following crashes. Three of these rates were following crashes due to plague: 1.466 (Biggins et al. 2006a, Fig 6.4), 2.024 (Cully and Williams 2001, Fig 4, years 1989-1991) and 3.806 (Cully and Williams 2001, Fig 4, years 1995-1997). We combined these rates with four growth rates following crashes due to other causes, including shooting, toxicants and removal and translocation (Reeve and Vosburgh 2006, Table 10-3, excluding the lowest and highest rates, which were from populations that had not undergone a recent population reduction). The average of these 7 exponential growth rates was 2.44. For sensitivity analysis, we used the quartiles, giving a range of 1.8 to 2.8. These values coincided with an independent estimate based on the intercept of the regression of population growth rate (R) on population size (N) from the data of Hoogland (1995, Table 16.1), which gave s estimates of 2.4 to 3.7, depending on the type of regression. Given that regression of R on N often overestimates R_{max}, this range is consistent with the estimate based on exponential growth phases of the two populations mentioned above.

We assumed each mapped colony (see above) represented a distinct biological population, with carrying capacity (K) defined as a function of colony area and average densities of prairie dogs. At Conata Basin, the average density of prairie dogs prior to the arrival of plague was 28.7/ha (Livieri 2006). Thus, we multiplied the number of cells in each patch with 7.175 (=28.7*0.25) to calculate the carrying capacity of that patch (because under the Ricker-type density dependence we used, average abundance would approximately equal the equilibrium abundance or carrying capacity). Colonies with K<100 were excluded from analysis, to decrease the number of populations and because very small populations do not contribute substantially to population dynamics. We assumed initial abundances were equal to K for

each population, and we ran a 10-year burn-in period for all simulations to ensure that all colonies were at equilibrium with their environment and had reached a stable age distribution.

Demographic structure and vital rates

We developed an age- and sex-structured matrix model for prairie dogs using RAMAS Metapop software (v. 6.0; Akçakaya and Root 2013), with eight female and six male age classes, parameterized using survival rates and fecundities drawn from Hoogland (2001). We parameterized the matrix according to a pre-breeding census. We used survival rates based on Hoogland (2001, Figs. 1a and 2a), and fitted a polynomial regression of survival rate vs. age for each sex to obtain a smooth function of age (Fig. S1-2). We calculated litter size as 3.1 (from Hoogland 2001, figure 3a). Combining this value with proportion of females breeding (0.43; Hoogland 2001), and survival rate of zero-year olds, we estimated fecundity as 0.418 daughters and 0.379 sons per adult female (age 2+) and 0.209 daughters and 0.189 sons per yearling female (age 1). We assumed polygynous mating system with each male mating with up to 4 females. Because the density dependence function modifies the stage matrix as a function of population size, the model results would be sensitive to the R_{max} value of the density-dependence function, not to the exact vales of survival rates and fecundities. Therefore, the sensitivity to vital rates was modeled through the R_{max} sensitivity (see section on sensitivity analysis, below). All colonies were initialized at K and at stable age distribution, and all simulations were run with a 10 year burn-in period (to reach approximate equilibrium in the prairie dog metapopulation).

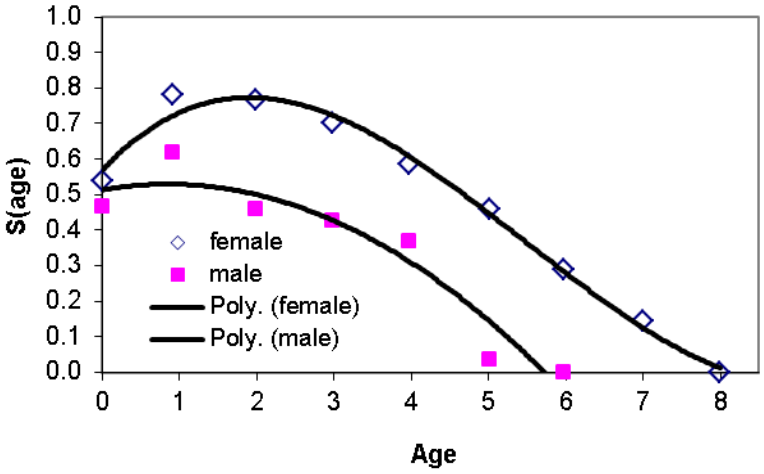

Figure S1-2. Illustration of polynomial regressions used to estimate expected age-specific survival rates for prairie dogs in this study, based on Hoogland (2001).

Variability

The temporal variation in vital rates is based on 14 years of age and sex-specific census data from Hoogland (1995, Table 16.1, page 377). It is important to note that the censused population has fluctuated between 150 and 250 individuals and does not seem to have crashed because of plague or other reasons during the study period (otherwise, adding disease dynamics would overestimate variability). In order to obtain environmental variability, we removed demographic variance from observed variance of survival rates and fecundities, based on expected binomial and Poisson variance

(Akçakaya 2002), and calculated coefficients of variation (Table S1-1). For sensitivity analysis, we used minimum and maximum values based on bootstrapping (Table S1-1).

Table S1-1. Coefficients of variation (CV) for survival rates and fecundities of males and females and minimum and maximum values of CVs based on bootstrapping

Vital rate	sex	CV	min CV	max CV
Survival rate	Female	0.111	0.102	0.119
	Male	0.185	0.136	0.201
Fecundity	Daughters	0.350	0.303	0.376
	Sons	0.291	0.268	0.331

Plague

We modeled plague dynamics within the prairie dog metapopulation as catastrophes spread by dispersers, with virulence (overall survival) and per-disperser probability of initiating an outbreak estimated from the Outbreak epidemiological model described below (n = 1000 replicates). We calculated the probability that a disperser initiates a catastrophe in the target population by multiplying the year-averaged probability that an individual (in a population that is experiencing an outbreak) is in disease state E (infected but not yet infectious), with the probability that a single individual in disease state E initiates an plague epizootic that kills at least half of the population. Specifically, the Outbreak model indicated a 9.3% chance of an individual disperser being capable of initiating plague in a new colony (averaged over an entire year, a prairie dog capable of dispersal from an infected colony had a 9.3% chance of being an exposed carrier), and a 97% chance that such a disperer would initiate a catastrophe, resulting in a 9% per-disperser chance of initiating a catastrophe. When a catastrophe does get initiated in a population, the survival rate is determined, according to the Outbreak results, as 2.9% survival (97.1% mortality) in the year that plague is initiated (with no long-term effects). We initiated the plague outbreak in year 11, following a 10-year plague-free period (in turn, following the 10-year burn-in period). reflecting ca. ten plague-free years at Conata Basin following the first ferret introductions (sylvatic plague was first detected in the Conata Basin in May 2008; Abbott and Rocke 2012). Plague was initiated in the prairie dog metapopulation assuming either (1) plague was initiated in a single randomly selected prairie dog population (selected from among mid size or larger populations in the Conata Basin), or (2) plague outbreaks arise spontaneously with a probability of 0.005 per year per colony (effectively resulting in spontaneous plague initiation events somewhere in the metapopulation nearly every other year). Because RAMAS Metapop computes the number of dispersers based on post-plague abundances, we also computed the mean number of infected (exposed) dispersers as a function of the final colony abundance, resulting in an estimate of 118% (SE 28%). Therefore, we set the "probability of infection per disperser" parameter in Ramas Metapop at its maximum value of 100% (thereby potentially underestimating the rate of spread).

Dispersal

Dispersal rates (proportion of individuals dispersing between each pair of defined populations) were modeled as a function of centre to edge distances between populations, in order to avoid very large populations flooding small populations around them. Dispersing prairie dogs traveled a mean straight-line distance of 2.4 km (Garrett and Franklin 1988). Maximum dispersal distance is 10 km (Knowles 1985 cited in Knowles et al. 2002; Lomolino and Smith 2001). Thus, we used a dispersal-distance function

$$a \exp(-D/b) = 0.083 \exp(-D/2.4),$$

where D is distance from the centre of the source population to the closest edge of the target population, with a maximum dispersal distance of D_{max} = 10 km. We calculated the intercept (the *a* parameter) as follows. Based on the spatial structure of populations, we calculated the average number of neighbors at distances of 0-0.5 km, 0.5-1 km, 1-2.5 km, 2.5-5 km and 5-10 km. We set the intercept such that the total expected rate of dispersal from this average population was about 0.37, which was calculated as the product of two numbers: (1) 59% of yearling males dispersing from a study population (based on data reported in Tables 1 and 2 in Garrett and Franklin 1988), and (2) relative survival rate of dispersers (calculated as 0.62, based on survival rate of 0.9 and 0.56 of residents and dispersers as reported by Garrett and Franklin 1988). For the spatial sensitivity analysis, we used a range of 0.061 to 0.105 for the *a* parameter, based on ± 0.10 for the total expected rate of dispersal from the average population.

The above calculation refers to dispersal rate of yearling males. We calculated the relative dispersal of other age/sex classes as 0.46 for yearling females, 0.1 for adult males and 0.39 for adult females (based on data reported in Tables 1 and 2 in Garrett and Franklin 1988). These numbers are consistent with general observations of age- and sex-specific dispersal: Hoogland (1995) reported that female prairie dogs usually remain with their natal coterie, or they disperse long distance to other colonies, but "short-distance dispersal of females within the home colony almost never occurs" (p.383); male prairie dogs, on the other hand, disperse either long-distance to new colonies (mostly as yearlings, rarely as adults) or short-distance within the home colony.

Correlation

Correlation of population dynamics among populations was based on a function of center-to-center distances between populations. Because annual fluctuations in vital rates are likely a function of weather conditions, we used temporal correlation in weather conditions as a proxy for describing correlation of population fluctuations. Specifically, spatial autocorrelation in vital rates was modeled as a function of inter-colony distances based on 30 years of summer rainfall data from 15 sites randomly drawn from within the range of the black-tailed prairie dog. We fitted a negative exponential model using 30 years of summer rainfall data drawn from 15 random locations in the southwestern quarter of South Dakota (PRISM dataset; PRISM Climate Group, Oregon State University, http://prism.oregonstate.edu). The resulting equation, correlation= exp(−*D*/601), where *D* is the distance between populations, was used for all model runs and was not modified as part of spatial sensitivity analyses (Fig. S1-3).

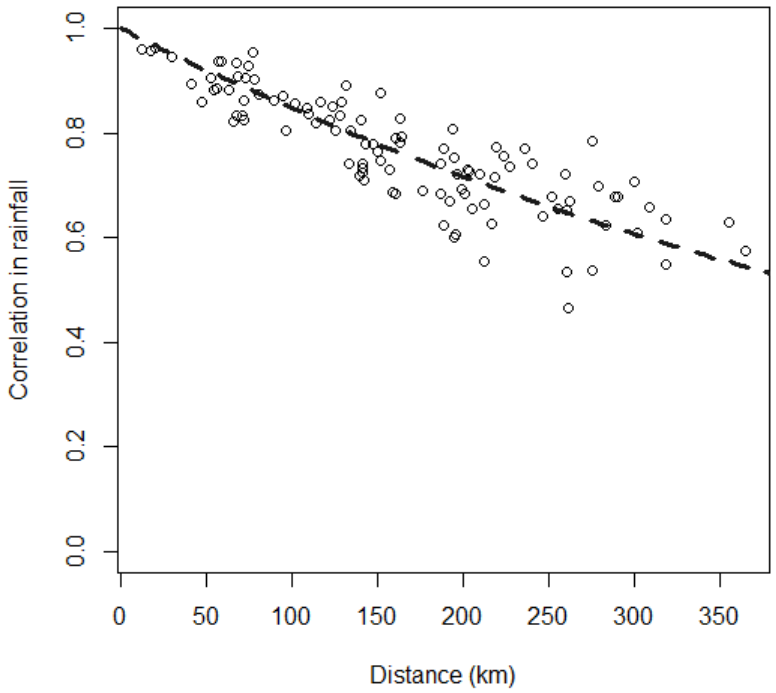

Figure S1-3. Illustration of the correlation-distance function used for all prairie dog models in this study. Spatial correlation in rainfall was assumed to correspond more generally to spatial correlation in environmental variation.

Black-footed Ferret Population Model

Demographic structure and vital rates

We developed an age- and sex-structured matrix model, with 5 female and 5 male age classes. We parameterized the matrix according to a post-breeding census, with survival rates drawn from a Wyoming mark recapture study (Grenier 2008). Juvenile (first year) and adult (yearling and above) survival rates were set at 0.39 (SE 0.17) and 0.67 (SE 0.15), respectively. For sensitivity analysis, we used a range of 0.22 to 0.56 for juvenile survival rate, and 0.52 to 0.82 for adult survival rate, representing one standard error from the mean. Juvenile and adult fecundity were set at 0.73 and 1.25, respectively, based on observations of kits produced from 2004-2006 (Grenier 2008). For sensitivity analysis, we used a range of 0.36 to 0.92 for juvenile fecundity and 0.86 to 1.35 for adult fecundity.

Density dependence, carrying capacity, and initial abundances

The strong dependence of Black-footed Ferrets on Prairie Dogs as prey suggests density dependence based on resource limitation and linked to resource (prey) dynamics. We therefore modeled Black-footed Ferret density dependence with a Ricker-type density dependence, corresponding to a scramble competition model (Brannstrom and Sumpter 2005).

We ran the black-footed ferret population model assuming either (1) ferrets could only access prairie dog colonies within the Conata Basin, or (2) ferrets could access all 1591 prairie dog colonies within the Conata/Badlands region. In the former case, we assumed the ferrets could only access PD colonies within the Conata Basin, a region of approximately 13,000 ha which we delineated as the aggregate of the three ferret subunits identified in Biggins et al. (2011). Thus, although the PD/plague model (see above) covered a larger area of southwestern South Dakota, only those populations in the Conata Basin were linked to the black-footed ferret model. Because ferret populations were rapidly extirpated by plague if limited to the Conata Basin proper, and because the maximum possible spatial extent for black-footed ferret populations is unclear (see main text), we also ran scenarios in which all prairie dog populations in the Conata-Badlands region were assumed to be available to the ferrets as prey.

We calculated the black-footed ferret numerical response based on the energy balance model of Stromberg et al. (1983), who concluded (via maximum sustainable yield computations) that a habitat area capable of supporting ca. 766 black-tailed prairie dogs was necessary to support the minimum energy requirements of a single black-footed ferret. We thereby equate a per-capita prey availability of 766 prairie dogs per ferret with a stable long-term ferret population growth rate (R = 1, corresponding to the carrying capacity in the scramble/Ricker density dependence function in RAMAS Metapop). Thus, carrying capacity (*K*) of the black-footed ferret population was calculated as 1/766 of the PD population size in Conata Basin at each time step. However, in years of high prairie dog abundance, ferrets typically maintain territories supporting more prairie dogs than they need to survive (Biggins et al. 2006b). In other words, the linear relationship between prairie dog density and black-footed ferret carrying capacity breaks down at high prairie dog densities. We capped the value of *K* at 462 for the Conata region based on the maximum ferret density of 0.04 ferrets per ha suggested by Biggins et al. (2006b). For global sensitivity analysis, we similarly capped the value of *K* to maintain a maximum density of 0.04 ferrets per ha (therefore, *K* varied based on landscape extent). Thus, even in years when prairie dog abundance is very high, the carrying capacity of the simulated ferret population does not exceed the maximum limit dictated by territoriality.

The energy balance model of Stromberg et al. (1983), upon which we based the functional linkage between ferret carrying capacity and prairie dog abundance (see above), assumed that ferrets fed exclusively on prairie dogs. However, a small but non-negligible component (ca. 10%) of the diet of the black-footed ferret is believed to comprise alternate prey items such as mice and lagomorphs (Campbell et al. 1987). The existence of alternate prey species raises the possibility that our models may overestimate the per-capita prey availability necessary to accommodate stable ferret population growth. However, prairie dogs are consumed by many species aside from the black-footed ferret (including badgers, bobcats, and coyotes; Hoogland 1995), raising the possibility that our model may underestimate the number of prairie dogs necessary to support a population of ferrets. Clearly, there is a great deal of uncertainty around this estimate, and we are planning a follow-up study to test the sensitivity of the ferret/prairie dog system to alternative characterizations of the functional and numerical response. Nonetheless, an estimated ferret carrying capacity of 485 at Conata Basin, computed as 1/766 of estimated total prairie dog carrying capacity, is consistent with the observed growth of the reintroduced ferret population at Conata Basin, which was beginning to plateau at abundances ca. 350 prior to the arrival of plague in 2007 (Livieri 2006; Fig. S1-4).

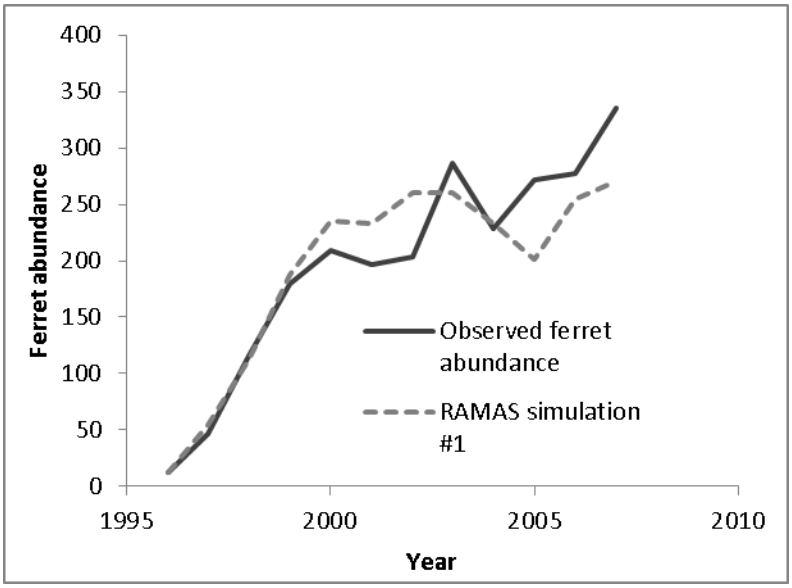

Figure S1-4. Observed abundance of black-footed ferrets at Conata Basin (from Livieri 2006), plotted alongside a single random replicate trajectory from the ferret population model , indicating the relative agreement between the observed growth of this population since ferrets were reintroduced in 1996, and the simulated trajectories from our model.

We set the maximum growth rate (R_{max}) to 1.48, based on the average of two estimates of the rate of (exponential) growth in a Wyoming population (Grenier et al. 2007). One estimate is 1.35, the eigenvalue of the matrix fitted to mark-recapture data, and the other estimate is 1.60, the (scalar) rate of growth in the minimum number of live ferrets from 2000 to 2006. For sensitivity analysis, we used these two values.

Black-footed ferret abundance for each iteration was initialized using known reintroduction events in the Conata Basin , as described by Livieri (2006; i.e., dates and ages of releases were modeled explicity). Ferret population viability was summarized using three metrics: quasi-extinction risk (defined as the proportion of simulation runs falling below 5 individuals at year 60 of the simulation), expected minimum abundance (defined as the minimum abundance after year 10 of the trajectory averaged over all 1000 simulations; McCarthy and Thompson 2001), and mean final abundance (at year 60).

Variability

We estimated temporal variability in ferret vital rates (i.e., variability not due to fluctuations in the prey base, which was modeled explicitly via variation in *K*) by running the linked ferret/prairie dog metamodel for Conata basin under plague-free conditions and adjusting the ferret temporal variability parameter to match the observed annual variability from the re-established ferret population in the Conata Basin (Livieri 2006; Fig. S1-4). Although most of the variability in black-footed ferret populations is likely due to variation in the prey base (here translated into variation in *K*), variability in other environmental factors may contribute to variability in black-footed ferret vital rates. To estimate the magnitude of this contribution, we created a retrospective model of the growth of the Conata Basin

black-footed ferret population from 1996 (shortly after its introduction) until 2007 (before the first plague outbreak) based on Livieri (2006). We reconstructed the Conata reintroduction effort using RAMAS Metapop, using management events (introduction and harvest) to schedule the history of ferret introductions and translocations described by Livieri (2006). We ran the simulations with demographic stochasticity, vital rates specified as above, and carrying capacity linked to natural temporal variability in plague-free prairie dog population density (see above). Variability in black-footed ferret population growth in the early years of the Conata reintroduction program was likely related to different release strategies and predator exclusion measures (Livieri 2006). Ferret releases largely ended in 1999, and therefore we assumed that population variability observed from 2001 through 2007 (prior to sylvatic plague epizootic) were due primarily to natural variability. Holding all other sources of variability constant (demographic stochasticity and variability in prey abundance), we adjusted the coefficient of variation for environmental variation in black-footed ferret vital rates so that the median simulated population variance (computed as the variance of (N_{t+1}/N_t), n = 1000 simulations) matched the observed variability in the Conata time series. The CV value that best fit the observed Conata time series (Fig. S1-4) was 11.5%, and this value was used to compute temporal process variation for all vital rates. For sensitivity analysis, the CV for ferret vital rates varied between 5 and 16%, which was the range of CV values for which the observed variability fell within the interquartile range from the simulations.

Sensitivity to uncertainty in vital rates

Sensitivity analysis results are not presented for the black-footed ferret population model, since the main objective of this project was to assess the sensitivity of the ferret population to plague dynamics across a variety of realistic prairie dog-occupied landscapes (see main text and Appendix S3). However, the simulation results were nearly identical across the plausible range of values for R_{max} and environmental variability (described above). This insensitivity of ferret extinction risk to ferret vital rates was due to the strong (nearly exclusive) dependence of ferret extinction risk on minimum landscape-level prairie dog abundance (see text; Fig. S4-6).

Appendix S2: Details of the plague transmission model used to inform plague spread among prairie dog colonies

Background

Sylvatic plague, caused by the bacterium *Yersinia pestis,* is an exotic vector-borne disease of wild rodents that was introduced to western North America near the start of the 19th century (Link 1955) and became widespread across the western states by the mid-1900s (Eskey and Haas 1940; Barnes 1982). It is now maintained in enzootic cycles within rodent populations throughout much of the semi-arid prairie biome (Barnes, 1993). This bacterium is highly transmissible by infected fleas (Poland and Barnes, 1979) and causes a rapidly fatal disease in prairie dogs (Barnes, 1993; Cully and Williams 2001). Since the arrival of plague, devastating epidemics in prairie dog populations have been described (Lechleitner et al, 1968, Gage and Kosoy 2005, Cully et al. 2010, Cully and Williams 2001, Ecke and Johnson, 1952). Plague epizootics occur variably every 5-10 years in affected prairie dog systems (Barnes, 1982) and can reduce colony size by >90% and disrupt mesocolony structure (Cully et al., 2010).

Sylvatic plague now affects much of the prairie region of the USA, presenting a clear challenge to the future of black-footed ferret reintroduction efforts (Livieri 2011). As the sole food source for the black-footed ferret, the impact of this disease on prairie dogs has limited the conservation of the black-footed ferret and consistently hampered attempts to reintroduce this endangered species to its former habitats. Consequently, control of plague outbreaks in prairie dog populations is an important conservation issue and has recently been incorporated into the Black-footed ferret Species Survival Plan (SSP).

We developed an individual-based epidemiological model based on comprehensive literature review of published field and laboratory data that simulated plague spread through a prairie dog colony (see below). Simulation of basic epidemiological processes and reporting of survival states was done at a daily time step using the software Outbreak version 1.0 (Pollak et al. 2008; Lacy et al. 2012). We used an Outbreak extension called Infector to accommodate plague spread through spatially structured prairie dog colonies (black-tailed prairie dog colonies consist of loosely connected collections of family groups, called coteries; Hoogland 2001). The capabilities of Infector have since been added to Outbreak version 2, available at www.vortex10.org/Outbreak.aspx. Outbreak models (n = 5000 iterations) were initialized with a single infected individual within a colony size of 1000 individuals, and all simulations were run for 365 days. Although there is some evidence for resistance to Y. pestis in black tailed prairie dogs (Rocke et al., 2012; Pauli et al. 2006), we chose not to model this because it is not yet well understood and therefore difficult to parameterize. Simulated epizootic dynamics and population outcomes were compared to known field observations of prairie dog populations in plague-endemic areas to validate the model. Outbreak output tables were used to generate three summary statistics that were subsequently used for modeling prairie dog metapopulation dynamics: (1) Overall survival rate in a plague outbreak year, (2) probability of a potential disperser individual being a carrier of plague, and (3) the probability of a single infected individual initiating a population-wide outbreak. Details of the Outbreak model are provided below.

Disease is introduced by initializing the population in Vortex, with one animal initially infected (disease state E), and all others susceptible. Hence, on day 1, an infected prairie dog (defined as exposed

in Outbreak) is introduced and becomes infectious after the required incubation period of 4-21 days. Once the individual transitions to infectious, s/he is capable of transmitting the disease agent and the plague outbreak is initiated. The dynamics of a plague epizootic are modeled as 365 days in Outbreak (with Infector). Vortex is used to initialize the population for MetaModel Manager (including disease state and coterie membership on an X-Y grid), but was not otherwise used in this initial model used to obtain disease parameters.

Initial population distribution among coteries (Infector specification)

Prairie dog coteries (family groups on a territory) are typically about 15 animals. The initial animals (*n* = 1000) were therefore assigned randomly to a 6x10 grid of territories. The exact age and sex distribution within these coteries does not affect the Outbreak model, because disease transmission was not modeled as being age or sex-dependent.

Disease transmission model

Transmission of *Y. pestis* was modeled as a combination of three different transmission mechanisms to capture the differential rates of disease transmission among coterie members, between adjacent coteries, and more distantly to prairie dogs in non-adjacent coteries.

- Transmission among coterie members was modeled with the "Within-group" transmission of Infector.
- Transmission between prairie dogs belonging to adjacent coteries (defined as those at X-Y coordinates within 1 in any direction from the focal coterie) was modeled with the "Between-group" transmission of Infector.
- Transmission between prairie dogs that are not in adjacent coteries was included within Outbreak.

An additional scenario was modeled to include transmission from a secondary reservoir such as grasshopper mice. The addition of grasshopper mice increased transmission between adjacent coteries and across longer distances between non-adjacent coteries but did not affect the within-group transmission rate.

Disease Parameters

Pre-susceptible

Q1 – Proportion that never become susceptible = 0

There is no evidence of life-long resistance to *Y. pestis* infection. However, evidence for reduced virulence over generational time scales is accumulating (Rocke et al. 2012), and such resistance will be included in future implementations of this model.

Q2 – Earliest age of susceptibility (days) = 1

Q3 – Latest age of susceptibility (days) = 2

There is no evidence of maternal immunity to *Y. pestis* in prairie dogs. Therefore, young are susceptible to infection immediately after birth and may become infected within the first couple days.

Transmission to Susceptible animals

Plague is spread between prairie dogs via fleas. When a diseased prairie dog dies, it is likely that its fleas would leave the carcass and seek other hosts nearby. Reported flea abundance differs pre- versus during/post-plague epizootic and has a wide range of reported values between studies. Environmental variables and climate (precipitation) drives flea populations, which in turn drives plague epizootics (Pauli 2006).

No plague: 39% pdogs harbor fleas with mean of 1.3 fleas/pdog (+/- 0.18)

Plague epizootic: 71% pdogs harbor fleas with 3.9 fleas/pdog (Tripp 2009)

No plague: 80% of pdogs infested with O. hirsuta; mean of 8.4-9.5 fleas/pdog

Plague epizootic: mean of 11.1 fleas/pdog

Fleas carrying plague can also be spread through the prairie dog population by the movement of diseased hosts (before they die- this is minimal), cannibalism/ contact with dead prairie dogs, infested fleas within burrows, or via the movement of other hosts, such as other rodents (grasshopper mice).

Overall prevalence of *Y. pestis* positive fleas found in prairie dog populations with plague activity is 12%. Prairie dogs infected with plague infect up to 93% of their fleas with *Y. pestis* (Engelthaler 2000), primarily during the terminal stages of the disease. Fleas collected from active prairie dogs captured in the colonies did not have *Y. pestis* positive fleas. Of fleas collected within burrows, 7% were infected with *Y. pestis*.

During plague epizootics 81% of grasshopper mice are infested with prairie dog fleas with a mean of 3.8 fleas/mouse. Mice within colonies with no plague activity have 1.6 fleas/mouse (Stapp, 2007). Unlike pdogs, grasshopper mice do not respect coterie boundaries so between coterie transmission and hence colony wide transmission is enhanced by the abundance of grasshopper mice driving epizootics . If dependant on pdog dispersal or annexation of neighboring coteries that have died from plague, infection will travel only sequentially to adjacent coteries and will not result in an epizootic.

The infectious state of fleas varies temporally with transmission probability of 0.416 on day 1, 0.111 on day 2, and 0.043 on day 3. Therefore, the farther that fleas travel before encountering a new susceptible host, the lower their infectious rate at the time of exposure.

Infector parameters:

Note: the capabilities of Infector have now been integrated into Outbreak version 2.0 (Lacy et al. 2012; available at www.vortex10.org/Outbreak.html).

Within-coterie transmission – To set the transmission rate within a family group, it was assumed that the fleas (mean 7.5; range 3.9 – 11) on an infectious (I) prairie dog would disperse from the infected host either as it was sick or when it died (over the span of three days). This would likely occur within the

burrow as *Y. pestis* is not transmitted to fleas until terminal stages of the disease. Active prairie dogs captured outside of burrows even during plague activity within the colony did not carry *Y. pestis* infected fleas (Engelthaler 2000). It was assumed that each coterie member has a 50% chance of receiving one of these infected fleas over the three days that the coterie member was infectious. Thus, the daily encounter rate was 1/6. This rate was then multiplied by the transmissibility of *Y. pestis* from infected fleas on the first day (0.416) on the assumption that transfer of fleas to a susceptible host would occur quickly within a coterie. This resulted in a daily transmission probability of 0.069333 within an infected coterie.

Between(adjacent)-coterie transmission – Two scenarios for transmission between adjacent coteries were evaluated. The first was solely dependent on prairie dog movement and annexation of a disease exterminated coterie by a neighboring coterie. It was assumed that naïve prairie dogs would enter a plague infected coterie from adjacent coteries once all prairie dogs in that infected coterie died from the disease. Given a coterie size of 15 and disease duration of two days, time to complete mortality of a coterie was estimated as 30 days following initial infection. To determine the contact probability for a neighboring prairie dog we used the encounter rate of 50% per day over three days that a prairie dog is infectious (1/6 per day) similar to the rate used in the within-coterie transmission. However, since a prairie dog would likely not enter a neighboring coterie until all members of that coterie were dead, we extended this probability over 30 days to get a daily encounter rate of 0.005556. We then multiplied this rate by the transmissibility of Y. pestis from an infected flea at two days post-infection (0.11) to get the probability of transmission between adjacent coteries by prairie dogs (0.0006111).

The second scenario included grasshopper mice as a transport host to achieve a higher rate of transmission of infectious fleas to adjacent coteries –similar to what has been demonstrated in the field and modeled previously (Salkeld et al. 2010; Webb et al. 2006). Grasshopper mice are not constrained by coterie boundaries and have been shown to visit multiple coteries within one day. We assumed an equal probability that one grasshopper mouse within an infected coterie territory would visit one of eight neighboring coteries per night, based on the spatial arrangement of the model. Once within a coterie, we assumed the mouse would encounter one prairie dog within that coterie (1/15). Combining these probabilities (1/15 * 1/8) gives the daily probability that one prairie dog encounters a grasshopper mouse. The proportion of mice infested with prairie dog fleas in colonies with plague activity has been reported at .81 and up to 93% of these may be infected with *Y. pestis* if acquired from a prairie dog carcass. Alternatively, if the fleas are picked up by elsewhere, the overall prevalence of *Y. pestis* associated in fleas is lower at 12% (Engelthaler 2000). Transmissibility of *Y. pestis* from an infected flea is considered to be 0.416 based on the assumption that grasshopper mediated flea transport will occur rapidly (within one day). Combining these probabilities [grasshopper mouse encounter (.00833) * proportion of mice infested with fleas (.81) * proportion of fleas infected with *Y. pestis* (.93) * transmissibility of the flea (.416)] results in a 0.00261 probability of transmission between adjacent coteries due to grasshopper mice. This probability was then added to the prairie dog associated transmission rate to generate a cumulative transmission rate of 0.00321 to model plague epizootics when grasshopper mice are included as a secondary reservoir.

Outbreak parameters:

Outbreak assumes that disease transmission is equally likely among any two animals in a population with no spatial structure to the disease spread. Therefore, Outbreak was used to model the transmission from an infected prairie dog to others elsewhere in the population, via transport of an infected flea by a

rodent (ie, grasshopper mouse) or other reservoir that was moving through the population. It was assumed that there was a 5% chance per day (i.e., 50 prairie dogs out of the 1000 in the prairie dog population per day) that a grasshopper mouse would encounter a prairie dog within three days of visiting a non-adjacent coterie. Upon encounter, there is a 0.81 probability that the mouse is infested with prairie dogs fleas, 12% of which may be infected with *Y. pestis*. We used the lower flea infection rate of 0.12 which reflects the overall prevalence of *Y. pestis* in fleas across a colony with plague activity (Engelthaler 2000). It was assumed that the infectiousness of the flea would have dropped to the lower 0.043 probability (3 days post-infection) by the time it found a distant host. [Note: the number of long-distance transfers of fleas seems very uncertain, but the overall disease dynamics is very insensitive to this parameter. Even if the rate is 10x higher, it will contribute rather little to the spread of the disease. The disease is maintained almost solely by the transmission between adjacent coteries.]

To model this scenario, the following Outbreak parameters were specified:

Q1 – Encounter rate was set as a fixed number (3) per day, rather than a proportion of the population, based on the number of coteries visited by a grasshopper mouse in one night (3) assuming that the mouse would encounter one prairie dog per coterie visited. This number is frequency dependent and thus would not increase with population size. Although the average encounter rate would be less than the 1 entered into the model, the lower rate was incorporated into the probability of transmission parameter.

Q2 – Probability of transmission = 0.00020898 (with 12% of fleas infected with *Y. pestis*) This value is from overall *Y. pestis* prevalence found in fleas collected in a prairie dog colony during plague epizootics (Engelthaler, 2000), and was calculated according to the following logic:

[Daily probability that a grasshopper mouse would encounter a prairie dog within three days of visiting a non-adjacent coterie (0.05) * proportion of mice infested with fleas (0.81) * proportion of *Y. pestis* positive fleas in a prairie dog colony during plague activity (0.12) * transmissibility of *Y. pestis* from flea on the third day post-infection (0.043)]

Q3 – Probability of encounter with an outside disease source = 0.0

We did not model any infection from sources that would be unrelated to the prevalence of plague within the prairie dogs themselves. Although some transmission might come from other species, the probability of such would likely be directly related to the prevalence of plague among the prairie dogs, and such transfer between host species could be subsumed under the model described above for transmission throughout the population.

Exposed

Q1 – Minimum incubation period = 4 days

Q2- Maximum incubation period = 21 days

Infectious

Q1 – Proportion that remain infectious indefinitely = 0. Prairie dogs infected with plague generally do not survive and there is no evidence for carrier states, therefore there is no probability that an individual will remain permanently infectious.

Q2 – Minimum infectious period = 2 days

Q3- Maximum infectious period = 4 days. Following development of clinical disease, prairie dogs usually die within 2-4 days.

Q4- Probability of recovery and becoming resistant = 0

Q5- Probability of returning to susceptible = 0.05. This value is calculated as 1- 0.95(probability of death) – 0 (probability of recovery).

Q6 – Probability of mortality from the infection = 0.95

Recovered/Resistant

Although some evidence for resistance to plague has been reported in prairie dogs (Rocke et al., 2012; Pauli, 2006), we chose not to include this in our model since it is not yet well understood and is therefore difficult to parameterize. For the purposes of this model, there is no recovery and acquired immunity among infected individuals so all values in this section were set to 0.

Appendix S3: Details of the sensitivity analysis routine

To investigate the effects of spatially-explicit plague dynamics on ferret population viability directly, we ran the ferret population model (1000 replicates each) with prey availability defined according to 500 distinct artificial prey landscapes (50 replicates each). Simulation settings were varied across the seven parameters hypothesized to most influence the dynamics of plague spread (and thereby affect ferret population viability), including four spatial characteristics related to landscape size and configuration, and three prairie dog demographic traits. Spatial variables were (1) total landscape size (square areas varying from 30 to 200 km per side), (2) number of distinct subpopulations (varying from 9 to 1681 separate colonies), (3) spatial clustering of colonies (colonies configured either in a regular grid or in 3 to 10 distinct clusters), and (4) background recurrence probability of plague (mean recurrence period varying from every 2 years to every 20 years within each landscape). Prairie dog demographic variables included in the sensitivity analysis were (1) maximum intrinsic rate of growth (varying from 1.8 to 2.8), (2) intrinsic dispersal rate (intercept term from Eq. 1, varying from 0.061 to 0.105) and (3) levelof temporal variability in growth rate. Each of the 500 scenarios was selected by randomly sampling a single value from within the low-high range for each uncertain parameter (Table S3-1). Duplicate scenarios were discarded and replaced to ensure that each simulation was unique. Total prairie dog abundance was evenly allocated across colonies such that landscapes with more colonies had lower per-colony abundances. Colony areas were determined by assuming a density of 50 prairie dogs per hectare (following typical estimates from high-density colonies; e.g., Severson and Plumb 1998) and colony overlap was not allowed. Clustered landscapes were created by specifying 3 to 10 starting locations and selecting neighboring colony locations according to a randomized algorithm that resulted in high-connectivity prairie dog complexes with widely varying sizes and shapes. To study the effects of spatial configuration and fragmentation *per se* (Fahrig 2003), initial abundance and carrying capacity were set at 2 million individuals (approximating the initial abundanc e of the Conata/Badlands region) for all scenarios, representing sufficient prey resources to support a robust population of over 2000 black-footed ferrets in the absence of plague (assuming a ratio of 766 prairie dogs per ferret). Given that all simulated landscapes were initialized with abundance and carrying capacity of 2 million prairie dogs, larger total metapopulation areas in our simulations corresponded to lower overall prey densities, with few to many (ranging from 9 to 1681) colonies spread evenly (grid) or unevenly (clustered) throughout the landscape.

We hypothesized that ferret extinction risk would be minimized for large, diffuse metapopulations, and that more frequent spontaneous reintroductions of plague within the prairie dog metapopulation would substantially reduce ferret population viability (Table S3-1). We assessed the relative importance of each variable as a predictor of black-footed ferret extinction risk using a distribution-free variant of the standard random forest algorithm (Breiman 2001) implemented using the `party` package in R (Hothorn et al. 2006; Strobl et al. 2007). Random forest is a general method for building multivariate predictive models that makes few assumptions about model structure or error distributions (Strobl et al. 2009). Relationships were visualized with conditional inference trees (Hothorn et al. 2006) and conventional bivariate scatterplots.

Because dispersal rates decline with the spatial separation of subpopulations, we may infer that mean nearest-neighbor distance (as a direct measure of connectivity) would be among the best predictors of plague spread, at least for gridded landscapes (the presence of clustered complexes makes this relationship less clear). Therefore, we also assessed the relationship between ferret extinction risk and mean nearest neighbor distance among prairie dog colonies. To test univariate associations and compare variables in terms of association with ferret population viability within the sensitivity analysis,

we also fitted univariate logit-linear models of black-footed ferret extinction risk as a function of each predictor variable. Univariate statistical models were fitted to the simulation output using maximum likelihood, and models were compared using the Akaike Information Criterion (AIC; Burnham and Anderson 2002).

Table S3-*1. Hypothesized influence of prairie dog variables on black-footed ferret (BFF) population viability*

Variable	**Possible values**	**Hypothesized influence on black-footed ferret (BFF) population viability**
Metapopulation size (number of distinct colonies)	9, 25, 81, 169, 441, 961, 1681	Greater number of colonies will correspond to higher BFF viability as predicted by metapopulation theory (e.g., Hanski et al. 1996)
Landscape size (km per side)	30, 40, 60, 80, 100, 200	Larger and more diffuse landscapes will correspond to higher BFF viability via lower connectivity and plague transmission rates (e.g., McCallum and Dobson 2002).
Spatial clustering of colonies	Gridded, clustered	Clustered prairie dog landscapes will enable persistence of ferrets in smaller landscapes than gridded landscapes, by reducing global connectivity (and thereby plague transmission) relative to an equivalent gridded landscape.
Mean period of spontaneous plague outbreak recurrence	2, 3, 4, 5, 10, 20	Presence of multiple plague initiation events (average of 1 colony every 2 years) will reduce BFF viability relative to single plague initiation event.
Intrinsic dispersal ability	0.061, 0.073, 0.083, 0.095, 0.105	Higher dispersal tendencies will result in more plague transmission events, and therefore will lower BFF viability.
Intrinsic (maximum) rate of growth	1.8, 2.0, 2.2, 2.4, 2.6, 2.8	Higher R_{max} will correspond to faster recovery from plague and therefore higher BFF viability.
Temporal fluctuations in vital rates	5 levels from low to high (see Table S1-1)	Higher temporal variability will not influence plague spread, but will increase risk of BFF extinction after plague episodes, when BFF (and prey) abundance is lowest.

After observing some unexpected, emergent oscillatory dynamics in the Conata landscape and in many of the artificial prey landscapes, we also examined how the seven key parameters influenced the emergence of oscillatory dynamics and the amplitude and frequency of the oscillations. We estimated the period of the dominant oscillation using sine wave regression (global prairie dog abundance modeled as an oscillating function of time) with coefficients estimated with maximum likelihood (results nearly identical to Fast Fourier Transform). Oscillatory amplitude was computed as the mean difference in abundance between significant peaks and troughs, which in turn were identified as 1-3 year time slices bounded by significant local (5-year) linear slope terms with opposite signs. Simulation scenarios

were categorized as strongly oscillatory if the sine wave regression model was selected over a standard linear regression as the best model (delta AIC > 2) for ≥ 75% of simulation replicates in a given scenario and the period of the oscillation was less than 50 years in length (Supporting Materials). To assess the potential role of plague-driven oscillatory cycles in destabilizing ferret populations, we also examined the correspondence between ferret extinction risk (and expected minimum ferret abundance) and the occurrence of oscillations.

Background rate of infection

Among the variables tested in the global sensitivity analysis was the landscape-level rate of plague recurrence (in years). However, the relevant parameter in RAMAS Metapop (Akcakaya and Root 2013) was the per-population (per-colony) rate of spontaneous reinfection (set using a .PCH file, which specifies the annual probability of catastrophe for each population; see Akcakaya 2005 for more details). We converted from the specified landscape-level background rate to the population-level background rate using the following equation,

$$br_p = 1 - (1 - br_l)^{1/ncols_l},$$

Where br_p is the population-level background rate of infection, br_l is the landscape-level background rate of infection (desired level set by the sensitivity analysis), and $ncols_l$ is the number of colonies in the landscape (also manipulated as part of the sensitivity analysis . The background rate of infection was set at 0 for the burn-in period (first 10 years) and the first 10 years of the simulation (representing the plague-free period in the Conata Basin).

Landscape configuration: clustered vs. gridded

In the spatial sensitivity analysis, the number of colonies was always set as the square of a real integer value (e.g., 9, 25, 81) such that all landscapes could be arranged as grids of prairie dog colonies with the number of colonies on each side computed as sqrt(# colonies). For prairie dog metapopulations with a grid configuration, the distance between nodes in the grid was set was computed by dividing the total extent of the landscape (km per side) by (# colonies + 1) (Fig. S3-1). Center-to-center distances between colonies (for use in determining the spatial correlation of environmental stochasticity) were computed using the Pythagorean theorem (colony centers were set at the internal nodes of the grid), and center-to-edge distances (for use in computing dispersal rates; see Appendix S1, section on Dispersal) were computed by subtracting the colony radius from the center-to-center distance. Assuming circular colonies, colony radius was computed according to the formula,

$$\sqrt{\left\{\left[\left(\frac{n_l}{ncols_l}\right)/d\right] * 0.01\right\}/\pi},$$

where n_l is the landscape abundance (set at 2 million), $ncols_l$ is the number of colonies in the landscape, and d is the maximum number of prairie dogs per ha, set at 50 per ha (see main text), and 0.01 is a conversion factor to convert from ha to km^2.

To explore the consequences of spatial aggregation of prairie dog colonies on plague spread and black-footed ferret population viability, we implemented the following clustering algorithm:

1) Divide the landscape into a fine grid
    a. Define distances between nodes (potential colony centers) such that the distances between the edges of potential colonies (assuming circular colonies with radii determined as above) are between 0.25 km and 2 km (selected randomly; typical range of inter-colony distances observed at Conata Basin study site). If the inter-colony distance is larger than that allowed by the landscape extent (determined according to the gridded colony configuration), then select a smaller inter-node distance that fits within the allowable landscape extent.
    b. Define the number of nodes per side based on the intended landscape extent (km per side divided by inter-node distance).
2) Randomly determine the number of clusters by sampling evenly from the set {4:10} .
3) Randomly determine the number of colonies in each cluster as a single multinomial draw with size set as the total number of colonies in the landscape and the probabilities assigned evenly across the number of clusters determined in the previous step.
4) Assign grid cells (uniform probability) randomly to serve as seed sites for cluster formation such that the distance between clusters is ≥10X the distance between colonies (center-to-center) where possible (constrained by the available the available landscape extent).
5) For each cluster, assign the locations of constituent colonies as follows:
    a. Beginning with the starting point (node) determined in the previous step, search for neighboring nodes that do not already host prairie dog colonies. Claim these nodes as the locations of constituent colonies.
    b. If some colony locations remain undefined and no neighboring nodes are available, randomly select a neighboring cell to serve as the new "starting location". Keep moving to new neighboring nodes until a node is identified such that at least one neighboring sites is available (currently unoccupied by a prairie dog colony).
    c. Repeat step (a), with the starting point replaced by the new focal node selected in (b).
    d. Continue until spatial coordinates have been defined for all colonies in the cluster
6) Once Cartesian coordinates have been defined for all colonies, determine center-to-edge distances (for estimating dispersal; see main text) and center-to-center distances (for estimating correlation of environmental variation) as described for gridded landscapes.

Using the center-to-center and center-to-edge distances between all pairs of colonies (gridded and clustered landscapes), dispersal and correlation matrices were computed in R following the equations presented in Appendix S1 and in the main text.

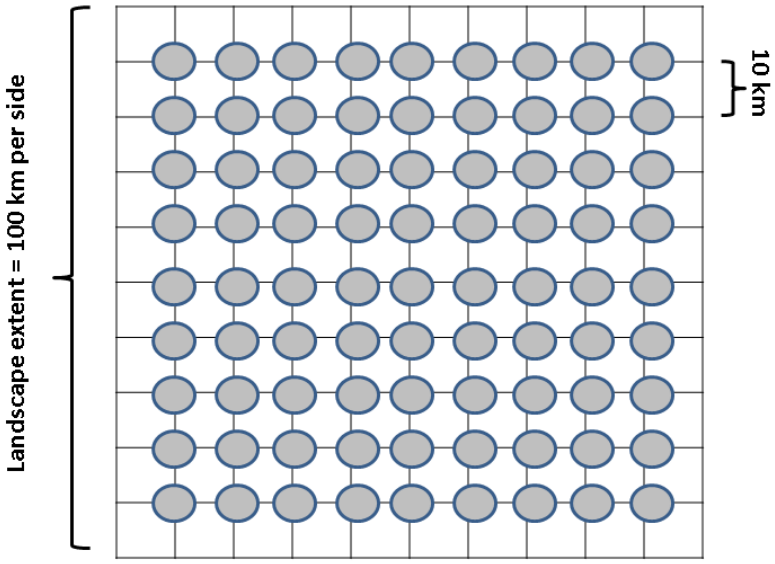

Figure S3-1. Illustration of the spatial arrangement of prairie dog colonies in the spatial sensitivity analysis. This illustration depicts a scenario with 81 colonies and a landscape size of 100 km per side.

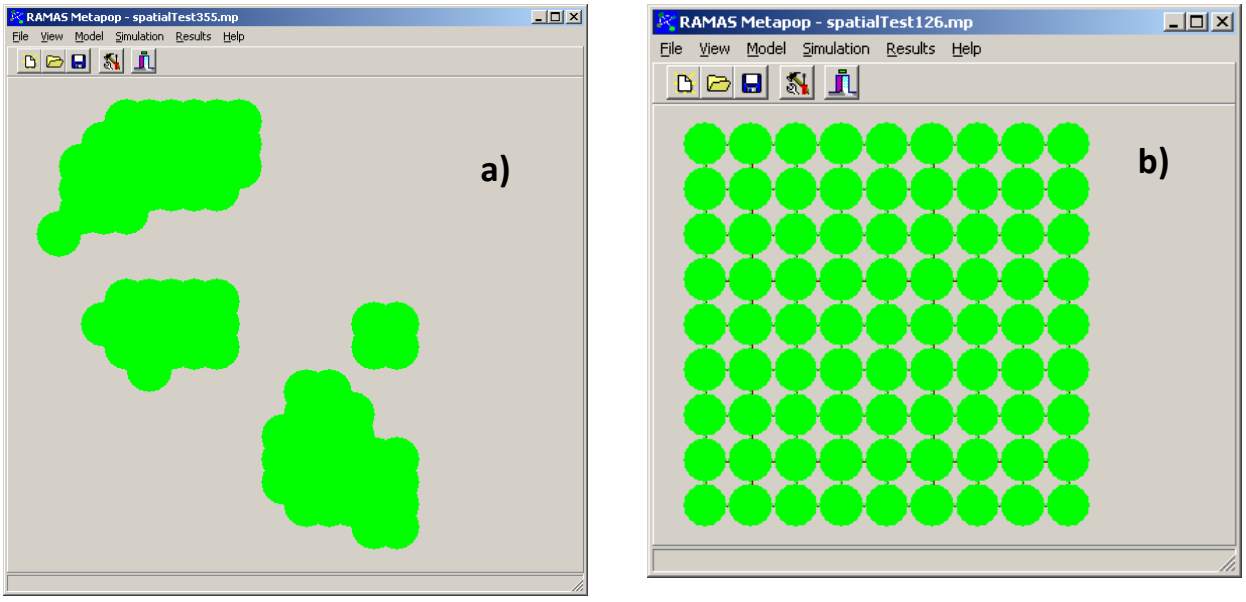

Fig. S3-2. Example of (a) a "clustered" prairie dog landscape with 81 colonies and (b) a "gridded" prairie dog landscape with 81 colonies, visualized in RAMAS Metapop software.

Temporal environmental variability

Sensitivity of black-footed-ferret populations to variations in the temporal environmental variability of prey populations was determined in the following way:

1) For each of four distinct prairie dog transition rates (male and female survival, production rates for males and females; Table S3-1), identify five coefficients of variation (CV) ranging from low to high, with low and high levels based on Table S1-1 and central (medium) variability value identical to the mean value listed in Table S3-1.
2) For each replicate scenario in the sensitivity analysis (n = 500), randomly select a value from 1 to 5 representing low to high temporal environmental variance.
3) For each of the four transition rates identified in (1), identify the CV corresponding to the variability level selected in (2).
4) Convert to standard deviations using the mean prairie dog transition rates (Appendix S1) and format as a matrix of standard deviations with the same dimensions as the transition matrix for exporting to RAMAS Metapop.

Details of the analytic approach for sensitivity analysis

Sine wave regression

We used sine wave regression to diagnose the presence of an oscillatory pattern and to identify the dominant period of the oscillatory pattern in years for individual simulation trajectories. Specifically, we fit the following 6-parameter model:

$$\log(N_t) = \beta_0 + \beta_1 \cdot t + \left(\frac{a}{2}\right) \cdot \sin\left(\frac{t}{\left\{\frac{p}{2\pi}\right\}}\right) + \left(\frac{z}{2\pi}\right) + e_t,$$

where N_t represents prarie dog abundance at time t, β_0 represents an intercept term (in log abundance units), β_1 represents a linear slope term (increase or decrease in log abundance each year), a represents the oscillatory amplitude, t represents time in years, p represents oscillatory period in years, z represents an offset term in years, and e_t represents a normally distributed iid error term.

For comparison as a null, non-oscillatory baseline model (with which to test the significance of the oscillatory pattern using a likelihood ratio test or AIC model comparison), we also ran an ordinary linear regression model (three parameters):

$$\log(N_t) = \beta_0 + \beta_1 \cdot t + e_t,$$

where t, β_0, β_1, N_t, and e_t are interpreted as above.

Model fitting was performed using custom likelihood functions in R with standard numerical optimization methods.

Identification of peaks and troughs

Although we describe the regular increases and decreases in abundances as oscillatory, in fact the periods between peaks or troughs were somewhat irregular within simulation runs (Fig. S3-3). Therefore, the peaks and troughs identified according to sine wave regression or Fast Fourier Transform (FFT) often did not adequately predict the true locations of peaks and troughs for a given abundance trajectory (Fig. S3-3). Therefore, we developed an *ad hoc* regression-based method for identifying peaks and troughs:

1) Define moving window parameter (number of years before and after a given year of the trajectory with which to define local trends). We used a 10-year moving window in this study to characterize local trends, corresponding to 5 years before and after the focal year (candidate for designation as a "valley").
2) Define the tolerance for Type I error (α). Following standard statistical practice, we set α at 0.05.
3) Define the minimum increase or decrease in abundance (over 0.5 * moving window parameter = 5 years in this study) necessary for designation as a meaningful change. In this study, we considered an increase or decrease of 100,000 individuals or more over a 5-year period as indicative of a meaningful change (populations were initialized at 2,000,000 individuals).
4) Loop through the trajectory (*n* = 100 years). For each focal year (buffered by 0.5 X moving window parameter),
    a. Run a linear regression of log abundance over the previous 5 years (0.5 X moving window parameter). Store the p-value associated with the slope term.
    b. Run a linear regression of log abundance over the subsequent 5 years (0.5 X moving window parameter). Store the p-value associated with the slope term.
    c. Using the above linear regression models, compute the expected change in abundance over the (5-year) relevant time window before and after the focal year and the sign associated with the change (increase or decrease).
    d. If the focal year meets the following criteria, then designate the focal year as a valley:
        i. P-value for the slope term over the window prior to the focal year must be less than or equal to the specified α.
        ii. The expected abundance over the relevant window prior to the focal year must decline by an amount greater than or equal to the value specified in (3)
        iii. At least one year in the relevant window subsequent to the focal year must be associated with a significant positive slope and a meaningful increase in abundance (see above).
        iv. No other valleys identified within the moving window.

a)

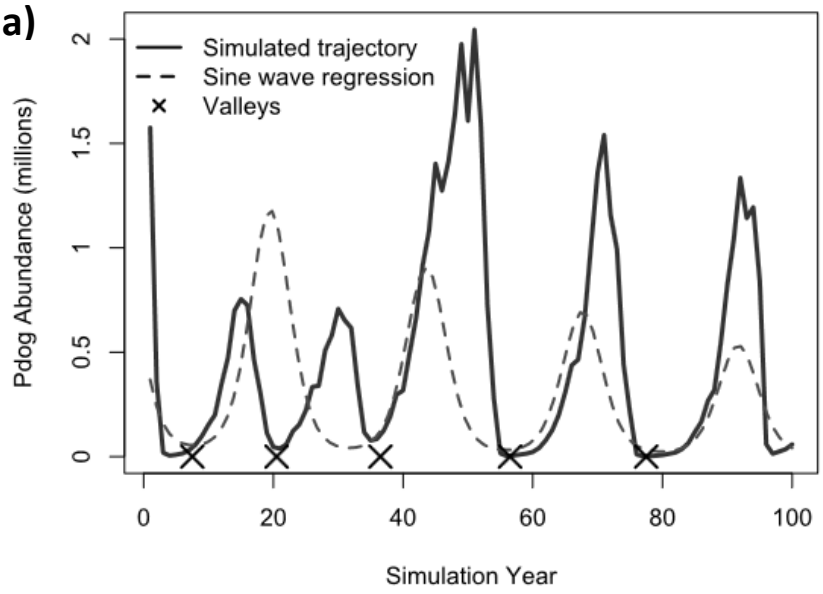
Simulated trajectory
Sine wave regression
Valleys
Pdog Abundance (millions)
0
0.5
1
1.5
2
0
20
40
60
80
100
Simulation Year

b)

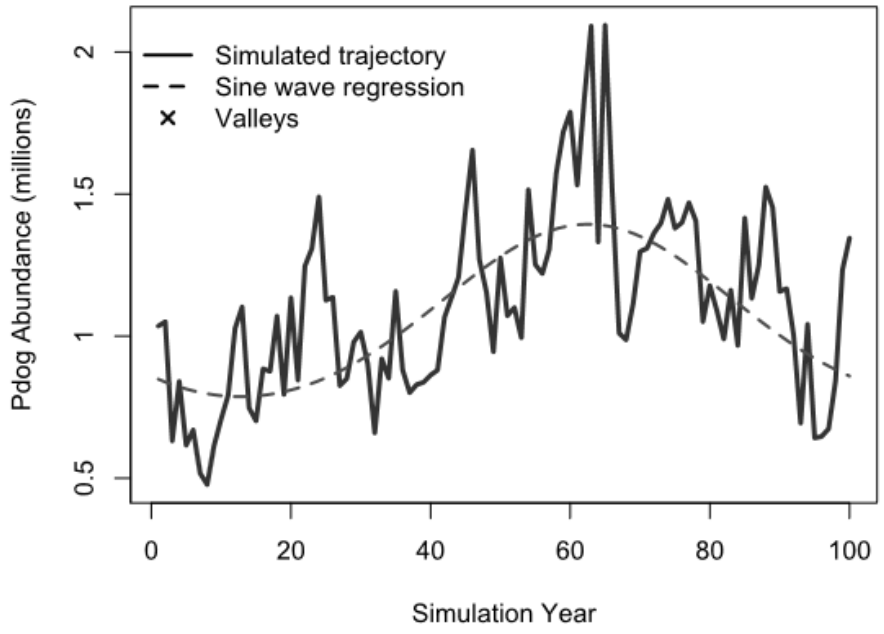
Simulated trajectory
Sine wave regression
Valleys
Pdog Abundance (millions)
0.5
1
1.5
2
0
20
40
60
80
100
Simulation Year

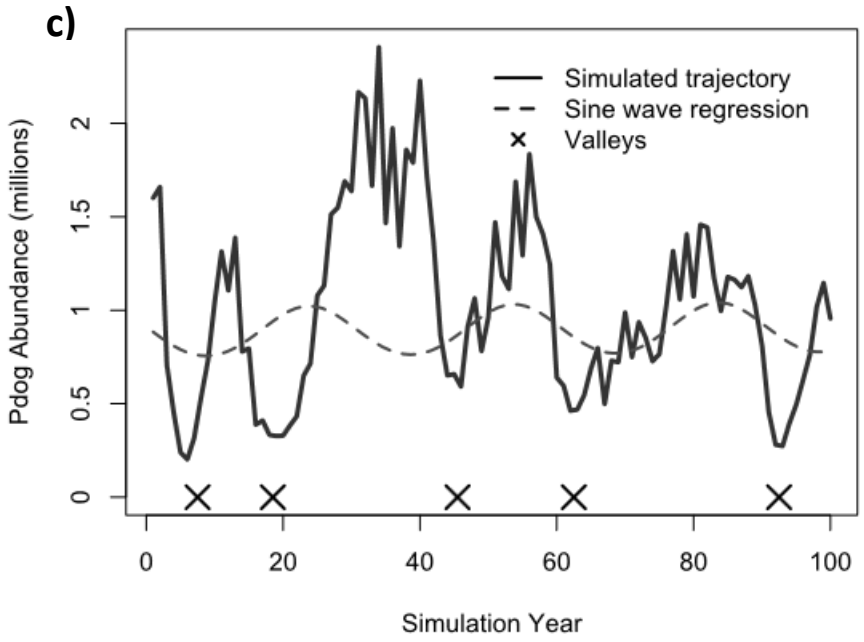

Figure S3-3. Illustration of the results of the sine wave regression and the valley identification algorithm for (a) a strongly oscillating scenario with 25 colonies with 40 X 40 km spatial extent and 5-year plague recurrence interval and (b) a non-oscillatory scenario with 169 colonies spread unevenly (clustered) in a 80 X 80 km landscape with 2-year plague recurrence interval (identified as non-oscillatory: no valleys identified and period of oscillation > 50 years) and (c) a weakly oscillatory scenario with 25 colonies distributed evenly (grid) within a 60 X 60 km landscape with a 2-year plague recurrence interval. Note that the sine wave regression did not accurately predict the locations of peaks and valleys nor did the amplitude of the sine wave regression accurately reflect the true difference in prairie dog abundance between peaks and valleys . In contrast, the regression-based algorithm was successful at identifying the true position of valleys and the true amplitude of the fluctuations.

Appendix S4: Supplementary Results and Figures

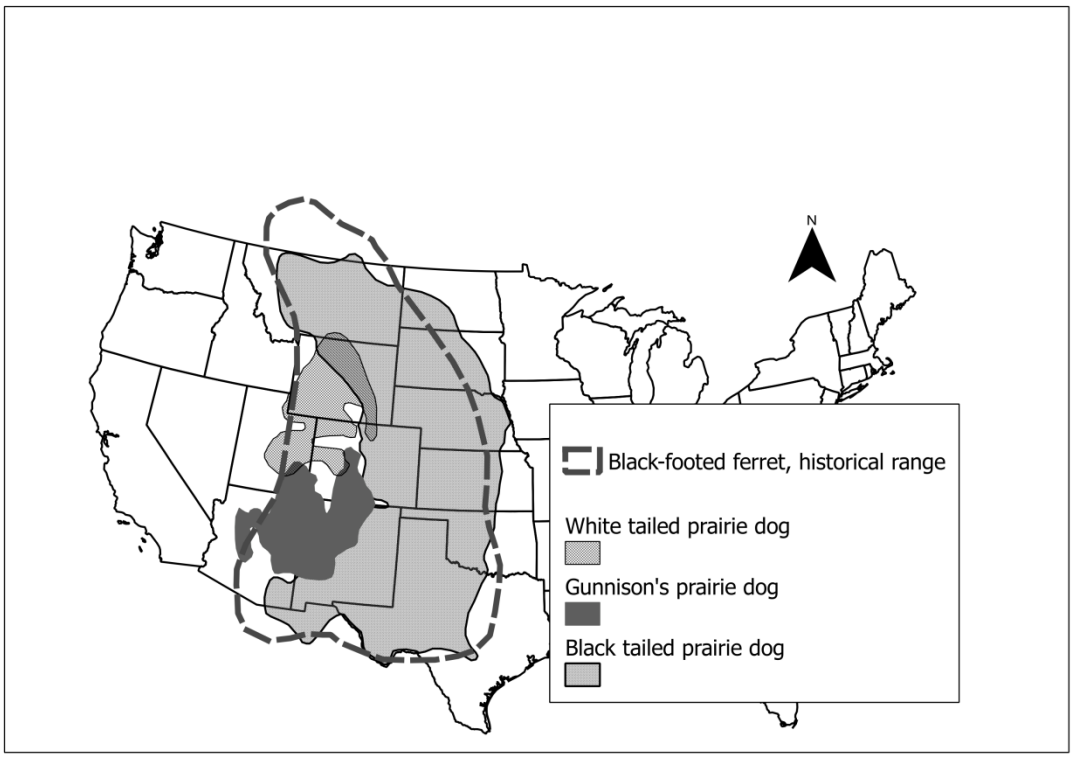

Figure S4-1. Historic range for the black-footed ferret,illustrated alongside the current ranges for the three species of prairie dogs historically consumed by black-footed ferrets (range boundaries obtained from NatureServe: http://www.natureserve.org/).

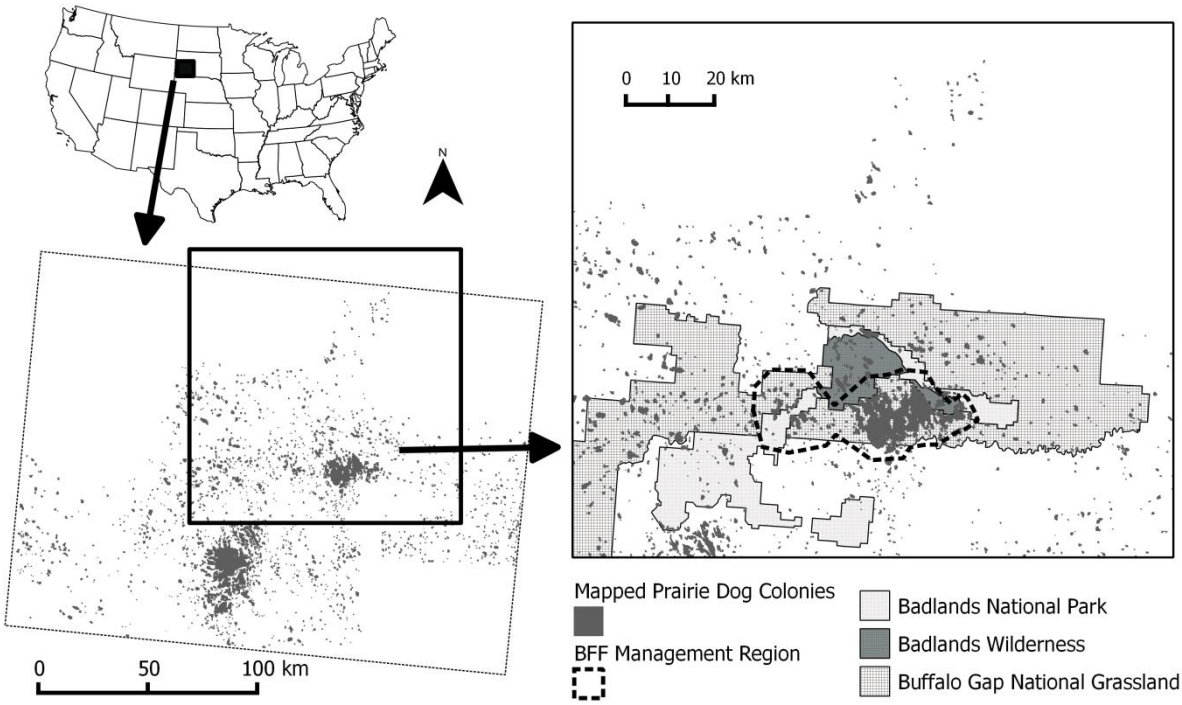

Figure S4-2. Map of the Conata Basin/Badlands study landscape (South Dakota, USA), depicting the locations of mapped prairie dog colonies, public lands, and the region of an ongoing black-footed ferret reintroduction program (the Conata region, labeled as "BFF Management Region").

Supplementary results: Conata Basin case study

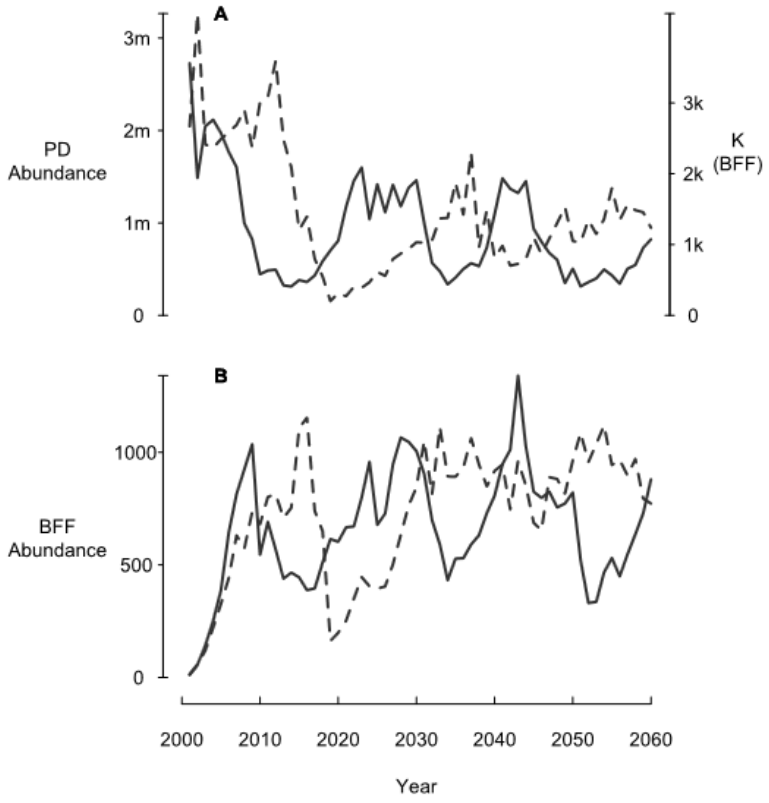

Figure S4-3. Example of oscillatory dynamics in (A) prairie dog abundance and (B) black-footed ferret (BFF) abundance that emerges as a consequence of plague spread within a vast complex of 1591 prairie dog (PD) colonies in the Conata/Badlands region, South Dakota, USA. Each of the two trajectories depicted (depicted as a solid and dashed line)represent single simulation replicates drawn randomly from 1000 replicate simulations. Because oscillations among replicate simulations were not in sync, the oscillatory pattern in mean abundance across replicates appears to dampen over time.

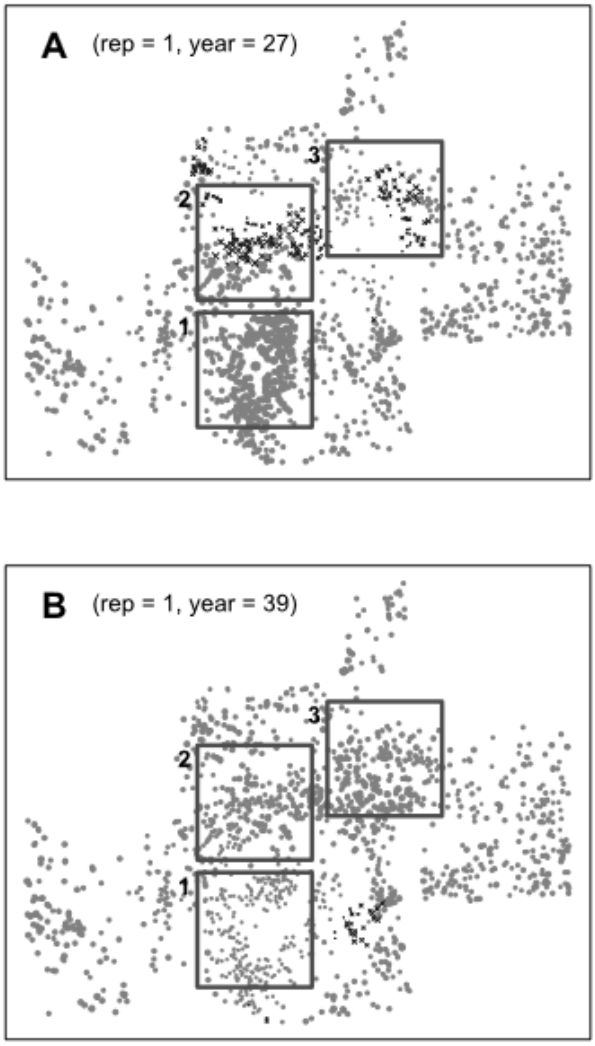

Figure S4-4. Illustration of the spread of sylvatic plague through the prairie dog population in the Conata/Badlands region. When plague is affecting a densely connected network of colonies within the region, other areas are recovering and capable of supporting black footed ferrets. The key to conservation in the face of plague may be to have enough spatial structure so that oscillatory plague outbreak cycles are asynchronous. This figure depicts two "snapshots" from a single replicate of the simulation model. Plague-affected colonies are illustrated with black X symbols; all other colonies are depicted as grey dots with variable sizes corresponding to abundances.

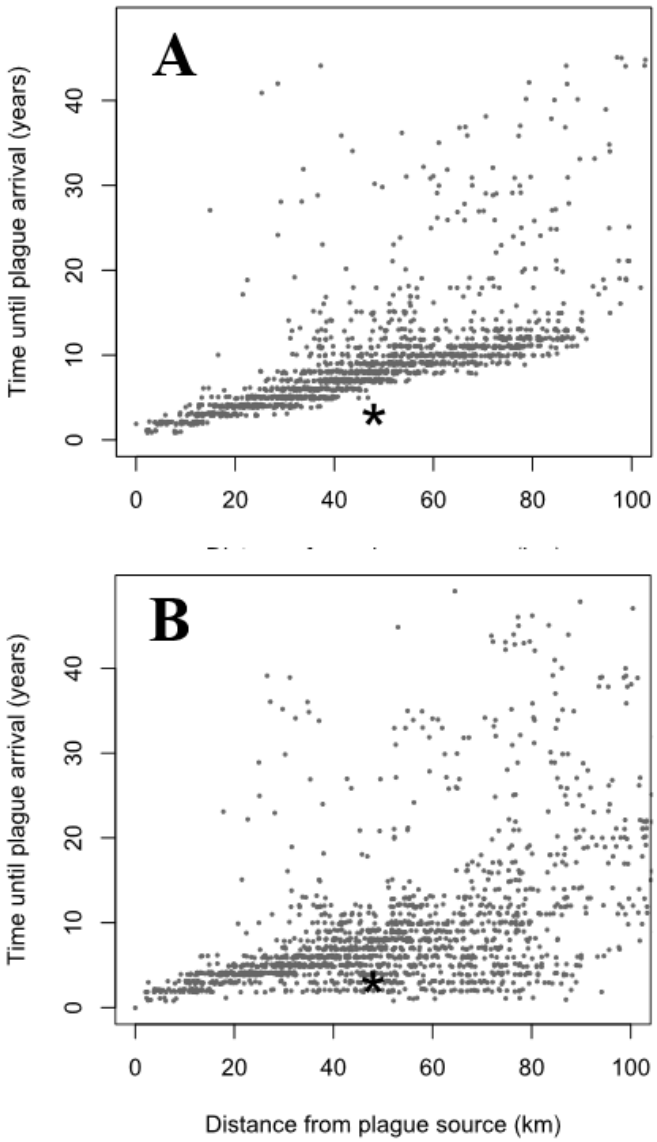

Figure S4-5. Timing of first plague event relative to distance from the site of initial introduction (A) with no background rate of infection (plague spread only by dispersing prairie dogs) and (B) with a 0.05% per-population probability of "spontaneous" plague infection (plague spread by alternative long-distance vectors such as coyotes). The asterisk in each panel represent the observed rate of spread at Conata Basin (T.M.L., unpublished data).

Animation of plague spread through the Conata-Badlands metapopulation

This animation presents the first ten replicates of the prairie dog metapopulation model (see text for details), each of which runs for 60 years. Each dot in the map represents the centroid of a black-tailed prairie dog colony in the Conata/Badlands region. The size of each dot scales with simulated colony abundance (log-transformed), and the colors indicate the occurrence (red) or absence (green) of a plague epizootic.

Link to animations: http://life.bio.sunysb.edu/ee/akcakayalab/PDog_simulation.htm

Supplementary results: sensitivity analysis

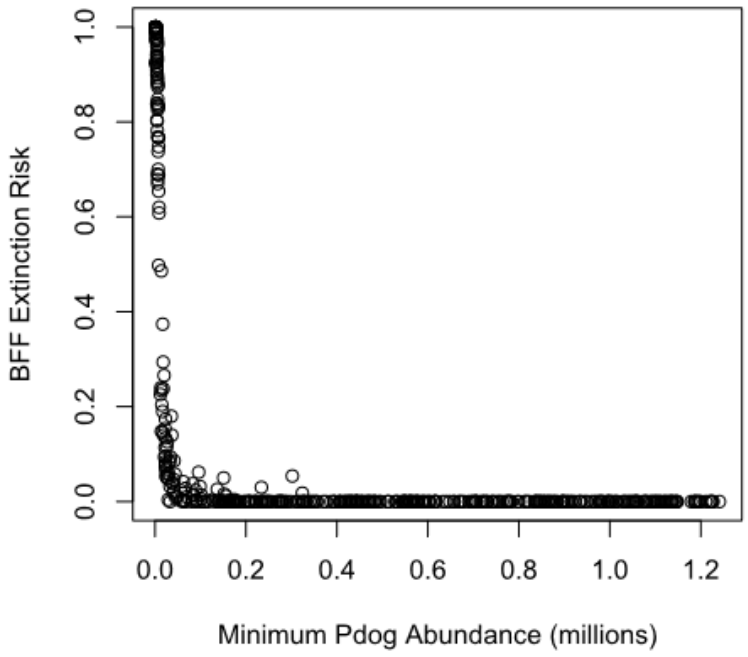

Figure S4-6. Illustration of the very tight relationship between black-footed ferret extinction risk and the expected minimum abundance of its obligate prairie dog prey

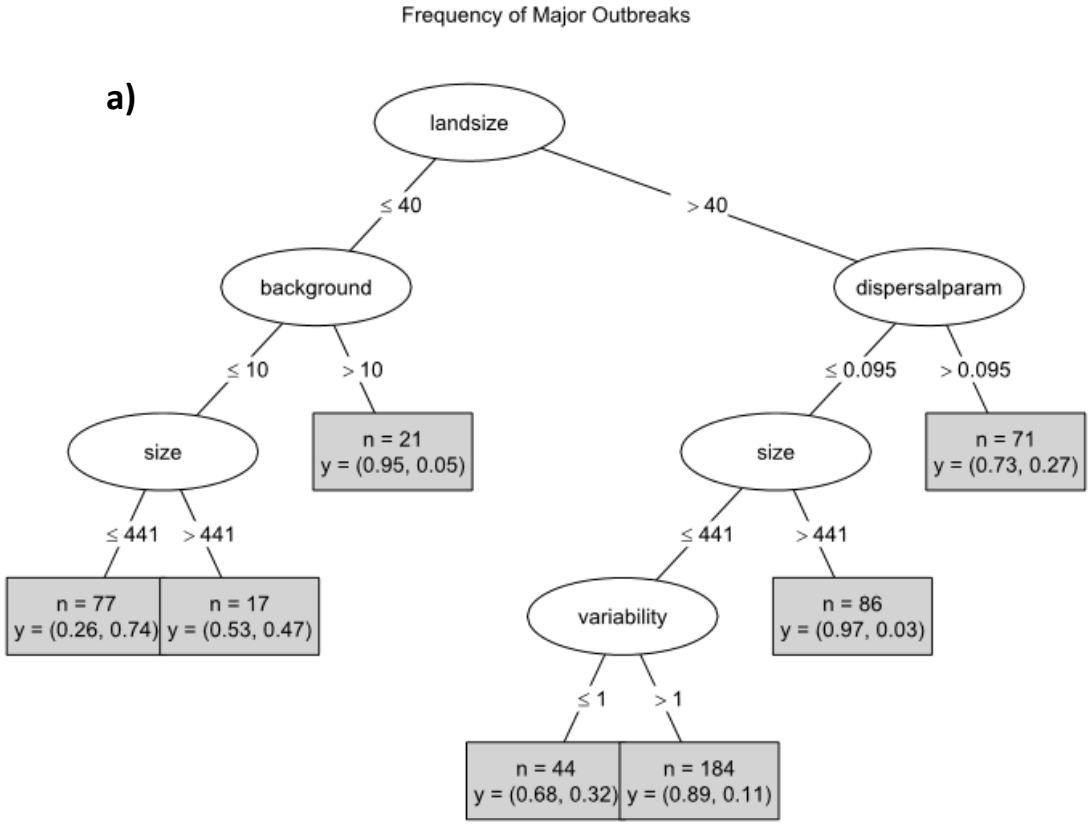
Frequency of Major Outbreaks
a)
landsize
≤ 40
> 40
background
dispersalparam
≤ 10
> 10
≤ 0.095
> 0.095
size
n = 21
y = (0.95, 0.05)
size
n = 71
y = (0.73, 0.27)
≤ 441
> 441
≤ 441
> 441
n = 77
y = (0.26, 0.74)
n = 17
y = (0.53, 0.47)
variability
n = 86
y = (0.97, 0.03)
≤ 1
> 1
n = 44
y = (0.68, 0.32)
n = 184
y = (0.89, 0.11)

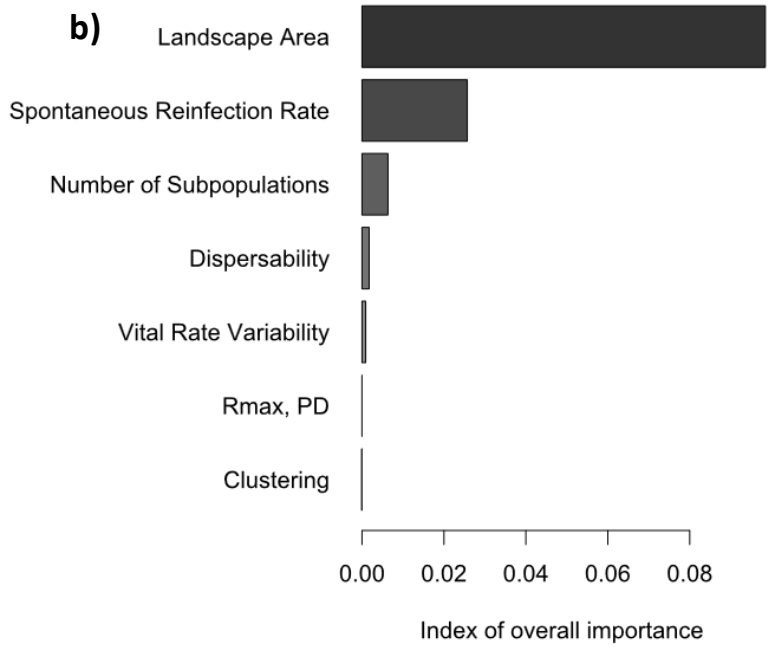
b)
Landscape Area
Spontaneous Reinfection Rate
Number of Subpopulations
Dispersability
Vital Rate Variability
Rmax, PD
Clustering
0.00
0.02
0.04
0.06
0.08
Index of overall importance

Figure S4-7. (a) Binary classifaction tree (conditional inference tree: party package in R) depicting the presence of a strong oscillatory pattern as a function of the sensitivity analysis variables. "landsize" is the landscape extent (km per side), "background" is the landscape-level period of plague recurrence (years), "dispersalparam" is the mean dispersal rate between adjacent prairie dog colonies, "size" is the number of colonies in the metapopulation, and "variability" is the magnitude of temporal process variance (low to high: 1 to 5). The shaded rectangles indicate the number of simulations represented by each leaf of the classification tree, along with the mean classification: the second value listed for "y" represents the frequency of strong oscillation. Therefore, strong oscillations were observed most often for landscapes with small spatial extent (≤40 km per side; corresponding to higher densities), frequent plague recurrence, and fewer than 450 colonies. (b) Indices of variable importance from a Random Forest model (conditional inference forest: `party` *package in R) depicting the relative importance of each sensitivity analysis variable in predicting the presence of strong oscillations.*

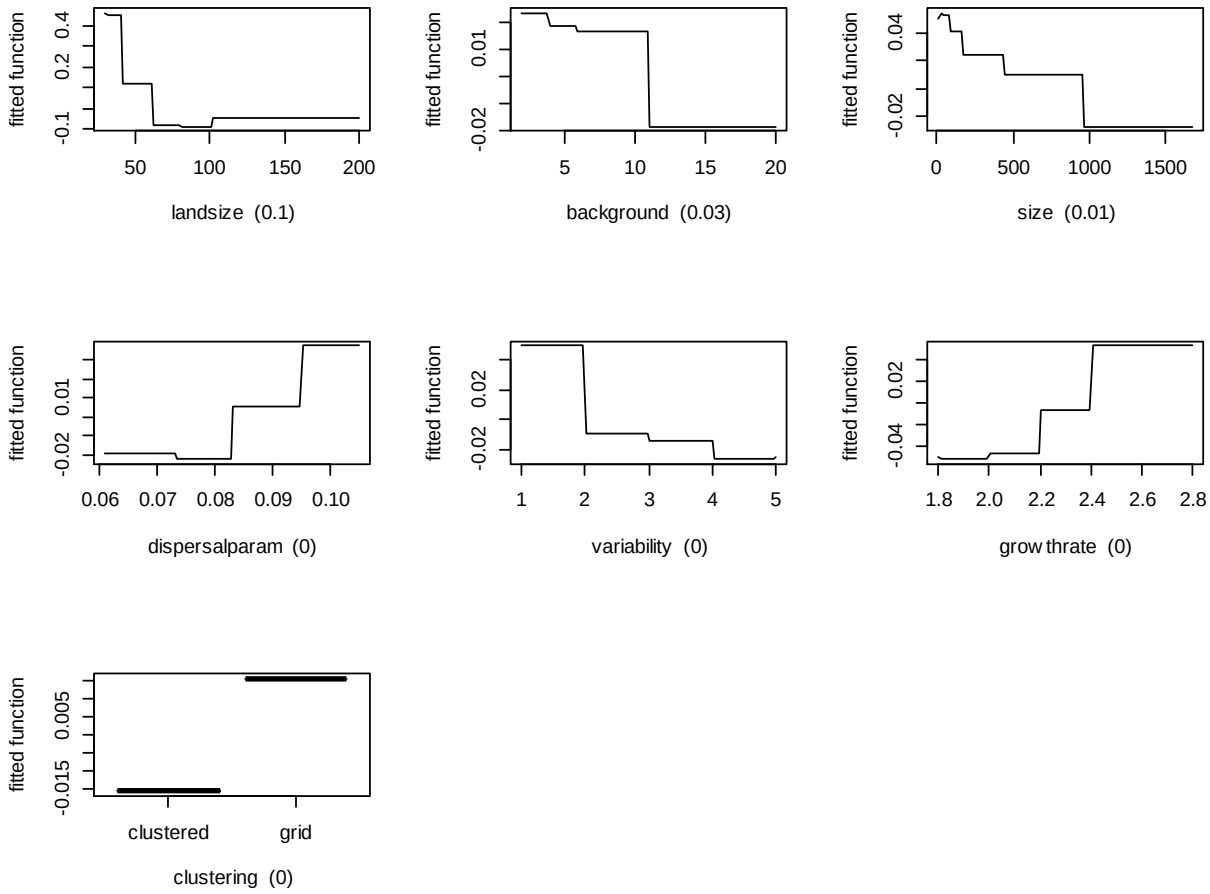

Figure S4-8. Univariate plots illustrating the overall effect of each of the seven sensitivity analysis variables on the frequency of a strong oscillatory pattern. Each plot is generated by using the Random Forest model to predict the probability of oscillation across the range of each sensitivity analysis variable, holding all other variables constant at their mean values.

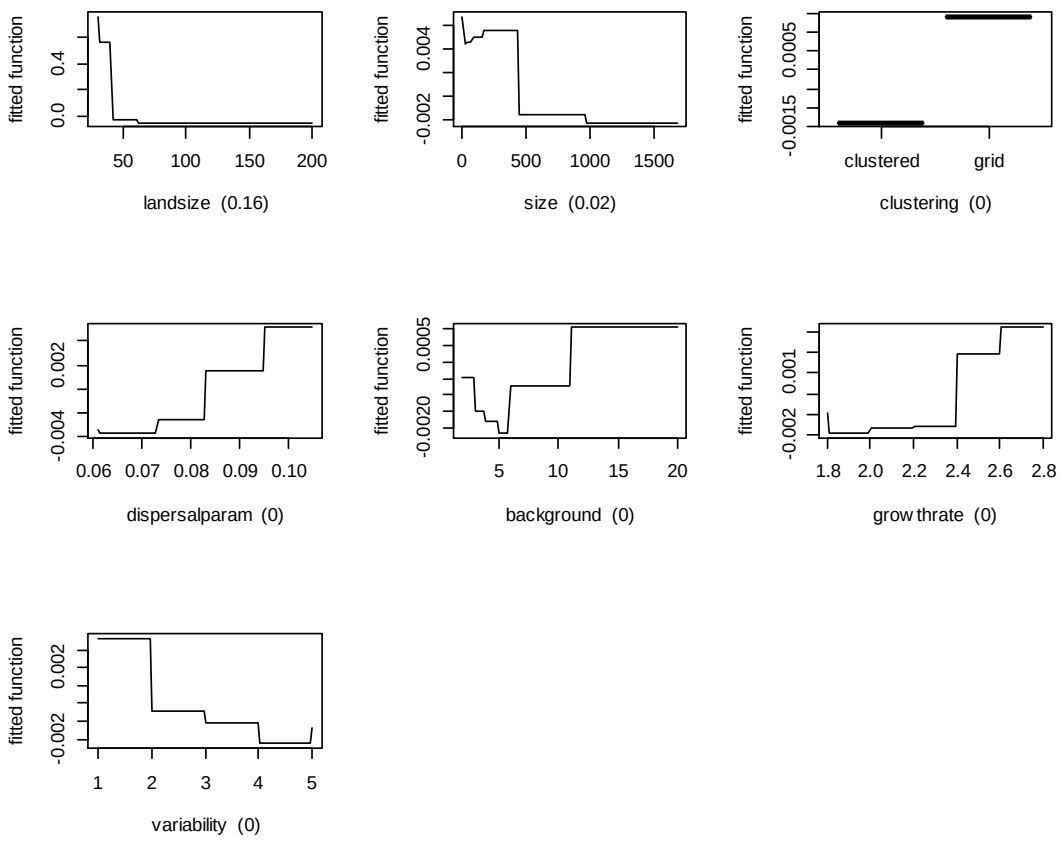

Figure S4-9. Univariate plots illustrating the overall effect of each of the seven sensitivity analysis variables on black-footed ferret extinction risk. Each plot is generated by using the Random Forest model to predict the probability of oscillation across the range of each sensitivity analysis variable, holding all other variables constant at their mean values. Note the strong similarity in the univariate responses of ferret extinction risk and the presence of a strong oscillatory pattern (compare with Fig. S4-8).

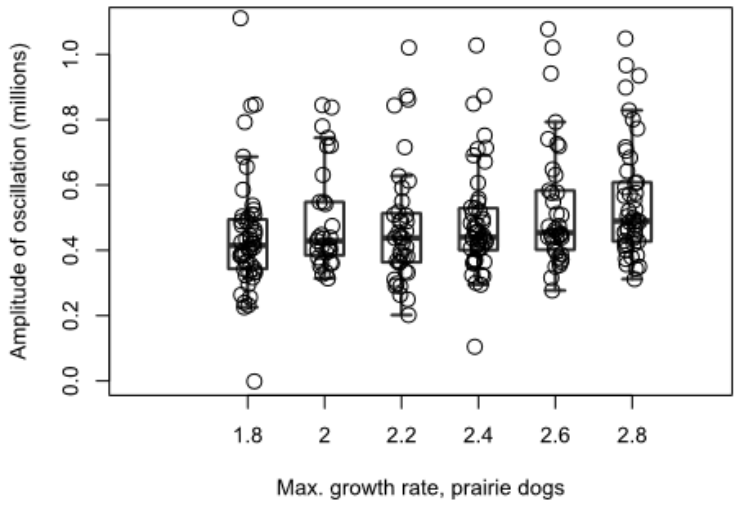

Figure S4-10. Illustration of a weakly positive relationship between maximum intrinsic rate of growth (R_{max}) for prairie dogs and the mean amplitude of abundance oscillations.

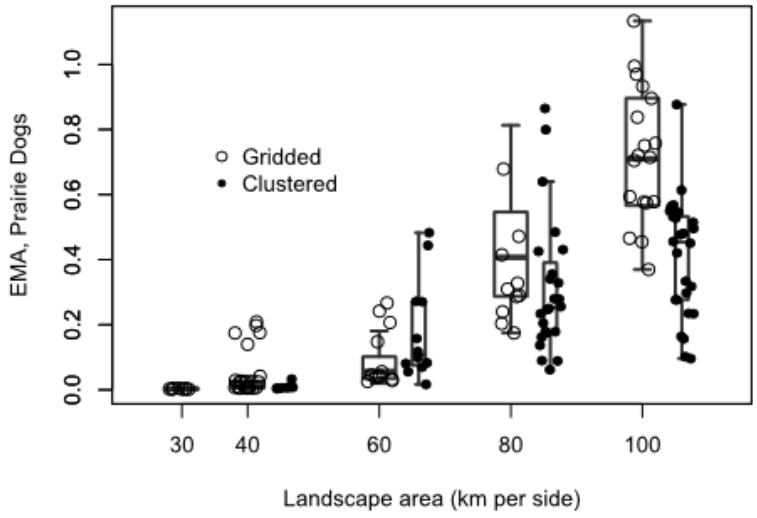

Figure S4-11. Visualizing the effect of landscape area and colony configuration (clustered or grid) on expected minimum abundance (EMA) for prairie dogs (in millions).

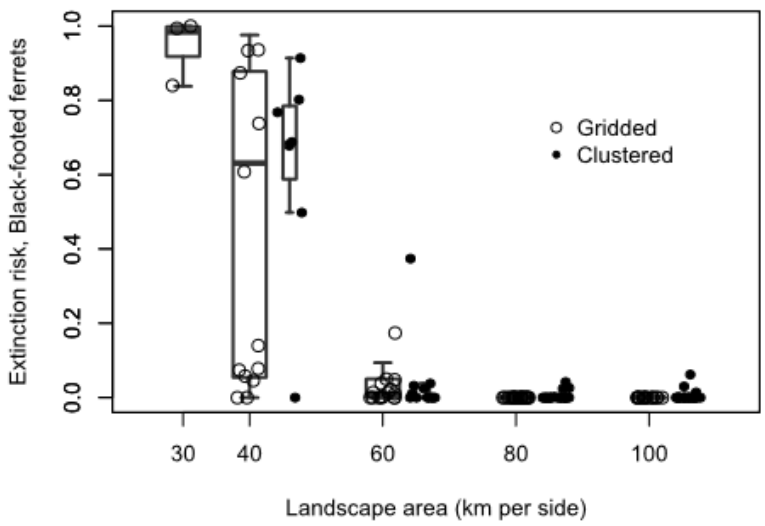

Figure S4-12. Theoretically, clustered prairie dog landscapes could provide some benefit for black-footed ferret conservation due to dispersal barriers. However, this effect was generally weak, and clustered landscapes in our simulation study were generally more likely to result in lower ferret viability due to large prairie dog complexes being devastated quickly and simultaneously.

REFERENCES

Abbott, R.C., & Rocke, T.E. (2012) *Plague: U.S. Geological Survey Circular 1372*, 79 pp., plus Appendix. (available at http://pubs.usgs.gov/circ/1372.)

Akçakaya, H.R. (2002) *RAMAS GIS: linking landscape data with population viability analysis* . Version 4.0. Applied Biomathematics, Setauket, New York.

Akçakaya, H.R. & Root, W. (2013) *RAMAS METAPOP: Viability Analysis for Stage-Structured Metapopulations*. Version 6.0. Applied Biomathematics, Setauket, New York.

Barnes, A.M. (1982) Surveillance and control of plague in the United States. *Animal disease in relation to animal conservation* (eds M.A. Edwards & U. McDonnell), pp. 237-270. Symposia of the Zoological Society of London 50. Academic Press, New York.

Barnes, A. M. (1993) A review of plague and its relevance to prairie dog populations and the black-footed ferret. *Proceedings of the symposium on the management of prairie dog complexes for the reintroduction of the black-footed ferret* (eds J. L. Oldemeyer, D.E. Biggins & B. J. Miller), pp 28-37. US Dept. Interior Biological Report 13. 96 pp.

Biggins, D. E, Sidle, J.G., Seery, D.B. & Ernst, A.E. (2006a) Estimating the abundance of prairie dogs. *Conservation of the black-tailed prairie dog: saving North America's western grasslands* (ed. J.L. Hoogland), pp 94-107. Island Press, Washington, DC.

Biggins, D.E., Godbey, J.L., Matchett, M.R. & Livieri, T.M. (2006b) Habitat preferences and intraspecific competition in black-footed ferrets. *Recovery of the black-footed ferret – progress and continuing challenges* (eds J.E. Roelle, B.J. Miller, J.L. Godbey, & D.E. Biggins), pp. 129-140. U.S. Geological Survey Scientific Investigations Report 2005-5293.

Biggins, D.E., Godbey, J.L., Horton, B.M. & Livieri, T.M. (2011). Movements and survival of black-footed ferrets associated with an experimental translocation in South Dakota. *Journal of Mammalogy,* **92**,742–750.

Brannstrom, A. & Sumpter, D.J.T. (2005) The role of competition and clustering in population dynamics. *Proceedings of the Royal Society B,* **272**, 2065–2072.
Breiman, L. (2001) Random forest. *Machine Learning*, **45**, 5–32.
Burnham, K.P. & Anderson, D.R. (2002). *Model Selection and Multimodel Inference: A Practical Information-Theoretic Approach*, second edn., Springer Science & Business Media, Fort Collins, CO.
Campbell, T.M., III, Clark, T.W., Richardson, l., Forrest, S.C. & Houston, B.R. (1987) Food habits of Wyoming black-footed ferrets. *American Midland Naturalist,* **117**, 208–210.
Cooper, J. & Gabriel, L. (2005) *South Dakota black-tailed prairie dog conservation and management plan*. South Dakota Department of Game, Fish and Parks and South Dakota Department of Agriculture, Pierre, South Dakota. 68pp.
Cully, J.F. & Williams, E.S. (2001) Interspecific comparisons of sylvatic plague in prairie dogs. Journal of Mammalogy, **82**, 894-905.
Cully J.F., Johnson, T.L., Collinge, S.K. & Ray, C. (2010) Disease limits populations: plague and black-tailed prairie dogs. *Vector Borne Zoonotic Disease,* **10**, 7–15.
Ecke, D.H. & Johnson, C.W. (1952) *Plague in Colorado and Texas. Part I. Plague in Colorado*. Public Health Monograph No.6. US Government Printing Office, Washington, DC. 37 pp.
Engelthaler D.M. & Gage, K.L. (2000) Quantities of Yersinia pestis in fleas (Siphonaptera: Pulicidae, Ceratophyllidae, and Hystrichopsyllidae) collected from areas of known or suspected plague activity. J *Medical Entomology,* **37**,422–426.
Eskey, C.S. & Haas, V.H. (1940) Plague in the western part of the United States*. U.S. Public Health Service, Public Health Bulletin,* **254**, 1-83.
Fahrig, L. (2003) Effects of habitat fragmentation on biodiversity. *Annual Review of Ecology and Systematics,* **34**,487–515.
Gage, K.L. & Kosoy, M.Y. (2005) Natural history of plague: Perspectives from more than a century of research. *Annual Review of Entomology,* **50**, 505–528.
Garrett, M.G. & Franklin, W.L. (1988) Behavioral ecology of dispersal in the black-tailed prairie dog. *Journal of Mammalogy,* **69**, 236–250.
Grenier, M.B. (2008). *Population biology of the black-footed ferret reintroduced into Shirley Basin, Wyoming*. Ph.D. Thesis, University ofWyoming, Laramie, USA.
Grenier, M.B., McDonald, D.B. & Buskirk, S.W. (2007). Rapid population growth of a critically endangered carnivore. Science, **317**, 779.
Hanski, I., Moilanen, A. & Gyllenberg, M. (1996) Minimum viable metapopulation size. *American Naturalist,* **147**, 527–541.
Hoogland, J.L. (1995) *The black-tailed prairie dog: social life of a burrowing mammal*. The University of Chicago Press, Chicago, Illinois.
Hoogland, J.L. (2001) Black-tailed, Gunnison's, and Utah prairie dogs reproduce slowly. *Journal of Mammalogy,* **82**, 917–927.
Hothorn, T., Hornik, K. & Zeileis, A. (2006). Unbiased Recursive Partitioning: A Conditional Inference Framework. *Journal of Computational and Graphical Statistics*, **15**, 651-674.
Knowles, C., Proctor, J. & Forest, S. (2002) Black-Tailed Prairie Dog Abundance and Distribution in the Great Plains Based on Historic and Contemporary Information. *Great Plains Research: A Journal of Natural and Social Sciences*, **608**, http://digitalcommons.unl.edu/greatplainsresearch/608 (accessed 23 May 2012).
Lacy, R.C., Pollak, J.P., Miller, P.S., Hungerford, L. & Bright, P. (2012). *Outbreak version 2.0.* IUCN SSC Conservation Breeding Specialist Group. Apple Valley, MN.
Lechleitner, R.R., Kartman, L., Goldenberg, M.I. & Hudson, B.W. (1968) An epizootic of plague in Gunnison's prairie dogs (*Cynomys gunnisoni*) in southcentral Colorado. *Ecology*, **49**,734-743.

Link, V. (1955) A history of plague in the United States. *Public Health Monographs* **70**, 1-120.
Livieri, T.M. (2006) *Ten-year history of the Conata Basin black-footed ferret population: 1996-2005.* Prairie Wildlife Research, Wall, South Dakota. 49pp.
Livieri, T.M. (2011) Black-footed ferret recovery in North America. *More Case Studies from Around the Globe* : *Global Re-introduction Perspectives* (ed. P. Soorae), pp. 157-164. IUCN/SSC Re-introduction Specialist Group, Abu Dhabi, UAE. 250pp.
Livieri, T.M. (2012) *Conata Basin Black-Footed Ferret Monitoring Report 2011-12 Season.* Report submitted to U.S. Forest Service – Wall Ranger Districs and Badlands National Park. Prairie Wildlife Research, Wellington, Colorado. 9pp
Lomolino, M.V. & Smith, G.A. (2001) Dynamic biogeography of prairie dog (*Cynomys ludovicianus*) towns near the edge of their range. *Journal of Mammalogy*, **82**, pp. 937–945.
McCallum, H., & Dobson, A., 2002. Disease, habitat fragmentation and conservation. *Proceedings of the Royal Society of London Series B,* **269**, 2041–2049.
McCarthy, M.A. & Thompson, C. (2001) Expected minimum population size as a measure of threat. *Animal Conservation*, **4**, 351–355.
Pauli, J.N., Buskirk, S.W., Williams, E.S. & Edwards, W.H.A. (2006) A plague epizootic in the black-tailed prairie dog (*Cynomys ludovicianus*). *Journal of Wildlife Diseases,* **42**, 74–80.
Poland, J.D. & Barnes, A.M. (1979) Plague. *CRC handbook series in zoonoses* (ed. J.H. Steele), pp. 515-597. CRC, Boca Raton, Florida.
Pollak, J.P., Miller, P.S., Lacy, R.C., Hungerford, L. & Bright, P. (2008) Outbreak version 0.99. IUCN SSC Conservation Breeding Specialist Group, Apple Valley, MN.
Reeve, A.F. & Vosburgh, T.C. (2006) Recreational shooting of prairie dogs. *Conservation of the black-tailed prairie dog: saving North America's western grasslands* (ed. J.L. Hoogland), pp. 139-156. Island Press, Washington, DC.
Rocke, T.E., Williamson, J., & Cobble, K.R., *et al*. (2012) Resistance to plague among black-tailed prairie dog populations. *Vector-Borne and Zoonotic Diseases,* **12**, 111-16.
Salkeld, D.J., Salathé, M., Stapp, P. & Jones, J.H. (2010) Plague outbreaks in prairie dog populations explained by percolation thresholds of alternate host abundance. *Proceedings of the National Academy of Sciences USA,* **107**, 14247-14250.
Sidle, J.G., Johnson, D.H. & Euliss, B.R. (2001) Estimated areal extent of colonies of black-tailed prairie dogs in the northern great plains. *Journal of Mammalogy*, **82**, 928-936.
Stapp, P. (2007) Rodent communities in active and inactive colonies of black-tailed prairie dogs in shortgrass steppe. *Journal of Mammalogy,* **88**, 241–249.
Strobl, C., Boulesteix, A.-L., Kneib, T., Augustin, T. & Zeileis, A. (2008). Conditional Variable Importance for Random Forests. *BMC Bioinformatics*, **9**,307.
Strobl, C., Malley, J. & Tutz, G. (2009) An Introduction to Recursive Partitioning: Rational, Application, and Characteristics of Classification and Regression Trees, Bagging, and Random Forests. *Psychological Methods,* **14**, 323-348.
Stromberg, M.R., Rayburn, R.L., & Clark, T.W. (1983) Black-footed ferret prey requirements—an energy balance estimate. *Journal of Wildlife Management*, **47**, 67–73.
Tripp, D.W., Gage, K.L., Montenieri, J.A. & Antolin, M.F. (2009) Flea abundance on black-tailed prairie dogs (*Cynomys ludovicianus*) increases during plague epizootics. *Vector-Borne and Zoonotic Diseases,* **9**, 313–321.
Webb, C.T., Brooks, C.P., Gage, K.L. & Antolin, M.F. (2006).Classic flea-borne transmission does not drive plague epizootics in prairie dogs. *Proceedings of the National Academy of Sciences USA*, **103**, 6236–6241.